FINAL REPORT

RUTGERS ZODIACAL LIGHT EXPERIMENT

on

OSO-6

Benjamin Carroll

Principal Investigator

December 10, 1975

Preface

During the winter of 1961 Dr. L. H. Aller visited Rutgers as a guest speaker for Sigma Xi. While visiting the polarmetry laboratory of Drs. A. L. Rouy and B. Carroll, Dr. Aller conceived the idea of the Rutgers zodiacal light experiment. Feasibility studies on the instrument followed for several years, the work being sponsored at first by the Space Institute located in New York. Subsequently NASA became interested in the Rutgers experiment. Their continuous encouragement and eventual sponsorship made this experiment possible.

The design of the flight instrument was based on the careful astronomical imput of Dr. Aller and the brilliant optical research experience of Dr. Rouy. From about 1955 Dr. Rouy had been engaged in my physical chemistry laboratory at Rutgers in the design of polarimeters for highly scattering systems. Six months after launching of the OSO-6 this project suffered a severe loss in the passing of Dr. Rouy-who had been the principal investigator. Dr. Aller and Carroll were the co-investigators at the time.

In the spring of 1970 Dr. Franklin E. Roach of Hawaii was invited to join this investigation, first as a consultant and finally as a co-investigator. His initiative, enthusiasm, and herculean efforts was a deciding factor in bringing this work to fruition.

During 1972-3 John R. Roach of Ball Brothers joined this investigation. Ball Brothers built the Rutgers instrument and John took a special interest in the

construction and performance of this instrument from the very beginning. Subsequently he contributed much effort in the astrophysical significance of the Rutgers data.

In preparing this final report each of the investigators was requested to contribute that section which I thought would do the most good. However the errors contained herein are those due to the editor.

Benjamin Carroll

Contents

1.0 RATIONALE FOR THE RUTGERS EXPERIMENT

In 1961, when LHA visited Rutgers University to give a Sigma Xi lecture, discussion turned naturally to the possibilities offered by rapidly developing space technologies to secure physical measurements that could not be obtained from the surface of the earth. Pointable telescopes were not yet in the offing, except for solar equipment. Accurate polarimetry and photometry was possible. Discussions between Carroll, Rouy, and LHA led us to examine the feasibility of securing accurate data on the surface brightness and polarization of the zodiacal light.

Since the days of the Cassinis, the zodiacal light had been explained as sunlight scattered by small particles circling in the inner solar system. In fact the outer solar corona, is seen at times of total eclipses arising primarily from light diffracted by these particles, but the surface brightness falls off rapidly with distance from the sun, partly because of the attenuation of the incident light, partly because of diminishing numbers of particles, and partly because of phase effects. Little was known about the particles, except that they were small, smaller than most telescopic meteors and had very low reflectivities. The material must be very transient in character as it is dragged rapidly into the sun by the Poynting Robertson effect.

A fundamental road block to the assessment and interpretation of the zodiacal light phenomenon and the character of the particles responsible was the poor quality of the basic observational data. It was not that capable astronomers had been negligent, indifferent, or lacking in perserverance. Teams of diligent

observers had gone to deserts in Africa, to the Canary islands, to the American SW, to Hawaii, and one hardy pair had risked their lives in the thin clear air of the high Bolivian Andes to secure good data. Yet, in spite of all of these efforts, plots of surface brightness as a function of angular distance from the sun and measurements of polarization showed staggering discrepancies. No theoretical framework could be erected in the quagmire of such discordances.

Why were the efforts of so many capable astronomers so grievously frustrated? The explanation is not hard to find when we realize that in its brightest portions (i.e. in the outer corona), the zodiacal light is tens of millions of times fainter than the sun. There, in its brightest portions it is difficult to observe even under the most favorable circumstances of a solar eclipse. In its outer portions its surface brightness drops by many orders of magnitudes and over most of the sky is in the neighborhood of 10^{-13} the surface brightness of the sun; hence it can be seen only under conditions of utmost sky clarity and freedom from moonlight or artificial light.

The zodiacal light extends over the entire sky and has an enhancement in brightness at the anti-solar point, called the counter-glow, contre-lumiere, or gegenschein, whose properties we will explore later in this report. The gegenschein is barely visible under optimum conditions on a dark, moonless, night in locations such as the Andes. The measurement of the surface brightness of the zodiacal light from the surface of the earth is very difficult. It is brightest, of course, near the horizon where one encounters all the usual

difficulties of atmospheric extinction (which dims it) and airglow which can falsely enhance its brightness. All modern measurements monitor the airglow, but the latter varies in intensity in position in the sky and in time. Away from the horizon and the ecliptic, where the surface brightness is low, one must substract the contribution of starlight (a particularly serious effect anywhere near the Milky Way). Polarization measurements are even more difficult because here one is concerned with subtracting two very small numbers, each of which is afflicted by large observational error. Thus, it is not surprising that different sets of published polarization data were not even qualitatively in accord with one another.

The arguments for measuring the zodiacal light above the earths atmosphere were thus compelling. One could escape all the uncertain corrections for atmospheric extinction and all the troubles imposed by a capricious airglow. In principle, at least, one could employ sufficiently long integration times to overcome the tyranny of small numbers and establish accurate data. However, one had to tailor the experiment to available or projected equipment - in other words the program had to be made compatible with a planned satellite experiment. Inquiry revealed that it would be possible to secure space for experiment to be flown in the wheel of an OSO satellite provided one could produce a viable experimental program.

Thus, it was necessary to obtain the boundary conditions of the experiment and then ask if -given these limitations- one could make scientifically worthwhile measurements? A detector placed in a slowly spinning wheel whose axis was perpendicular to the line drawn to the sun, could measure surface brightness and

polarization at all elongations from the immediate neighborhood of the sun to the anti-solar point.

As the axis of the wheel gradually turned in the course of a year, eventually the whole sky could be covered. From the known order of magnitude brightness of the zodiacal light at all points in the sky it was possible to calculate the feasibility of making measurements with different wavelength settings and polarizations, with the eventual goal of obtaining Stokes parameters for selected elongations from the sun. It was possible to define a program of orderly measurements involving a systematic use of different filters, polarimeter settings and integration time to obtain statistically reliable counts for each choice of these parameters, and covering all significant elongations. Details of the experimental phase are given in chapters 3 & 5. For the present it is sufficient to say that the measuring sequence was arranged to give longer integration times for the regions of lower surface brightness and that calibration was arranged via an attenuator that reduced the intensity of sunlight by a known factor, and via stars which were caught in the sweep of the device across the sky. This system provided a check on any possible deterioration of the system or any bogus polarizations that might be introduced by the optical system.

Although the experiment was conceived in 1962, and planned in detail in the following couple of years, it was not to be flown until 1969. Accordingly, there was time to undertake a theoretical program designed to suggest ways in which the measurements could be utilized to try to answer some fundmental problems concerning these particles. At UCLA in 1963, B. J. O'Mara coded the Mie

theory for the IBM computer. He, S. J. Little, and LHA then constructed models for the zodiacal clouds, utilizing both Mie theory for spherical particles and scattering functions derived from aerosol experiments by Richter. An attempt was made to determine size distribution, density variation, and number variations, the albedo, and to discriminate between metallic and dielectric particles. A comparison of Richter's results with those predicted for the same particle size distribution with a Mie distribution was made to ascertain how far the Mie theory might be applied to nonspherical aggregates. This calculation showed that the then existing zodiacal light data permitted a wide range of solution in particle size distribution, density distribution, etc. for reasonable choices of dielectric materials, and that the metallic component was small (Astron. Journal, 70, 346, 1965). A more ambitious program was then undertaken by a UCLA team of 9 participants who calculated the Mie scattering properties for spherical particles whose size distribution was given by a power law, whose spatial distribution varies smoothly with solar distance but whose optical properties did not change with distance from the sun. (Zodiacal Light Symposium 1967; NASA SP-150). They attempted to predict colors, isophotes and isopolarization contours, concluding that: a simple power law form, a^{-p}, will not work unless p assumes different values above and below a critical limit (b) the color of the zodiacal light may change with position in the sky, (c) the particles may thin out in number near the sun, (d) the index of refraction is low (metals and most dielectrics would appear to be excluded), and (e) small solid dielectrics can be retained in the system, but lower limits exist for sizes of metallic or carbon particles and fluffy particles of any kind. They

would simply be blown out by radiation pressure.

This extensive theoretical program, most of the cost of which was not born by NASA, but rather by UCLA, was undertaken not only from the light particles, but also and more significantly for the following reason which was not mentioned in the publications.

The observable quantities are intensities and polarizations at different positions on the celestial sphere. The object of the game is, given such data what can we ascertain about the nature of the particles, size distribution, probable composition, number etc. It is quite clear that measurements in some positions of the sky will be much more important than others.

Of course it is no surprise that the most significant measurements pertain to domains where the surface brightness is low and polarization is difficult to find. In the region between elongations of 145° and 180°, the polarization sign changes for many dielectric substances. We hope we can infer the character of the particles from such clues, from their albedoes, and color indices.

Further investigations treated situations in which the optical properties of the materials changed with distance from the sun, particularly the albedoes decreased as one approached the sun. In the absence of an appropriate physical theory, it is difficult to set the leeway in the choice of parameters. Results obtained with these models involving particles of variable blackening have not been published.

Unfortunately, preliminary trials by laboratory simulation of possible light

reflection effects caused by the nearby illuminated earth were never carried out before the experiment was flown. Throughout most position angles, light scattered into the detector from the parts of the space craft illuminated by the earth overwhelmed the zodiacal light signal so that the only valid measurements are those made near the antisolar point when the satellite is near the shadow of the earth, emerging or entering. It is unfortunate that the satellite was not designed so that measurements could be made during satellite night, as then we could have measured the zodiacal light over all elongations from 90° to 180°. The polarizmeter, itself, worked superbly well, as described below.

2.0 THEORY OF INSTRUMENT DESIGN

The Rutgers instrument has been adequately described in the BBRC Final Report, F70-11 and will not be repeated here. We consider instead several problems related to the optical design. Additional aspects of the Rutgers instrument are considered in the following sections.

2.1 Preliminary Considerations

The function of the Rutgers polarimeter was to describe at various elongations, the zodiacal light, its total brighiness, degree of polarization, ellipticity and the orientation of the plane of polarization (or major axis) with respect to a selected set of coordinates in the spacecraft, being in this case with reference to the spin axis of the vehicle. Light intensity measurements were made available so that transformation from the laboratory to celestial coordinates was possible. The author has encountered at least four different reported treatments on the Rutgers instrument. These will be critically reviewed here.

The analysis of a partially elliptically polarized beam of a given frequency (circular and linear polarization being taken as special cases of elliptical polarization) require four orientations of an optical analyzer in addition to two using a retarder and an analyzer. (See Bonn and Wolf: Principles of Optics 2nd ed. Macmillan Co. New York 1964.) Obviously a convenient set as suggested by Bonn and Wolf and upon which the Rutgers instrument is based is orthogonal pairs of measurements. In the case of the Rutgers instrument the effective

settings of the pass-axis of the analyzer (Rouy prism) may be written as

$$[0^\circ, 0]\ ,\quad [90^\circ, 0]\ ,\quad [45^\circ, 0]\ ,\quad [135^\circ, 0]\ ,\quad [0^\circ, \tfrac{\pi}{2}]\ ,\quad [90^\circ, \tfrac{\pi}{2}]\ .$$

where the angles are reckoned from the spin axis, the second numeral in the brackets representing the phase shift of the retarder. (Here we assume the fast axis of the retarder is set at right angles to the spin axis.) The above sequence will subsequently be referred to as positions 1 to 6 respectively.

Since some of the problems can be understood better by considering the actual number of optical elements involved for each position, the operational settings are listed in table 2.1. The arrangement of optical elements are shown in figure 2.1 taken from BBRC Final Report F70-11. There are six modes for a particular color. The instrument having three color filters restricting the spectral bandpass to an interval of approximately 400A centering around, 4,000, 5,000, and 6100A yields a total of eighteen readings for a given elongation. Actually the number is ninety since each reading is repeated five times in order to improve precision.

The fact that each of the six settings have different kind and number of optical elements i.e. position 1 and 2 contain a single rotator in the optical path whereas position 3 and 4 contain two rotators and 5 and 6 contain a rotator and quarter-wave plate raises the problem of the effective transmission for the six modes as affected by absorption, reflection, and scattering. The latter could become increasingly significant with the gradual deterioration of these elements in space.

Table 2.1 *

Position	Wheel 1	Wheel 2	Effective Position Analyzer Pass Axis with Respect to Spin Axis
1	-45° Rotator	Clear	0°
2	+45° Rotator	Clear	90°
3	+45° Rotator	+45° Rotator	45°
4	-45° Rotator	+45° Rotator	135°
5	-45° Rotator	$\frac{\lambda}{4}$ Plate	-
6	+45° Rotator	$\frac{\lambda}{4}$ Plate	-

*The analyzer pass axis is fixed at 45° to the spin axis of the spacecraft.

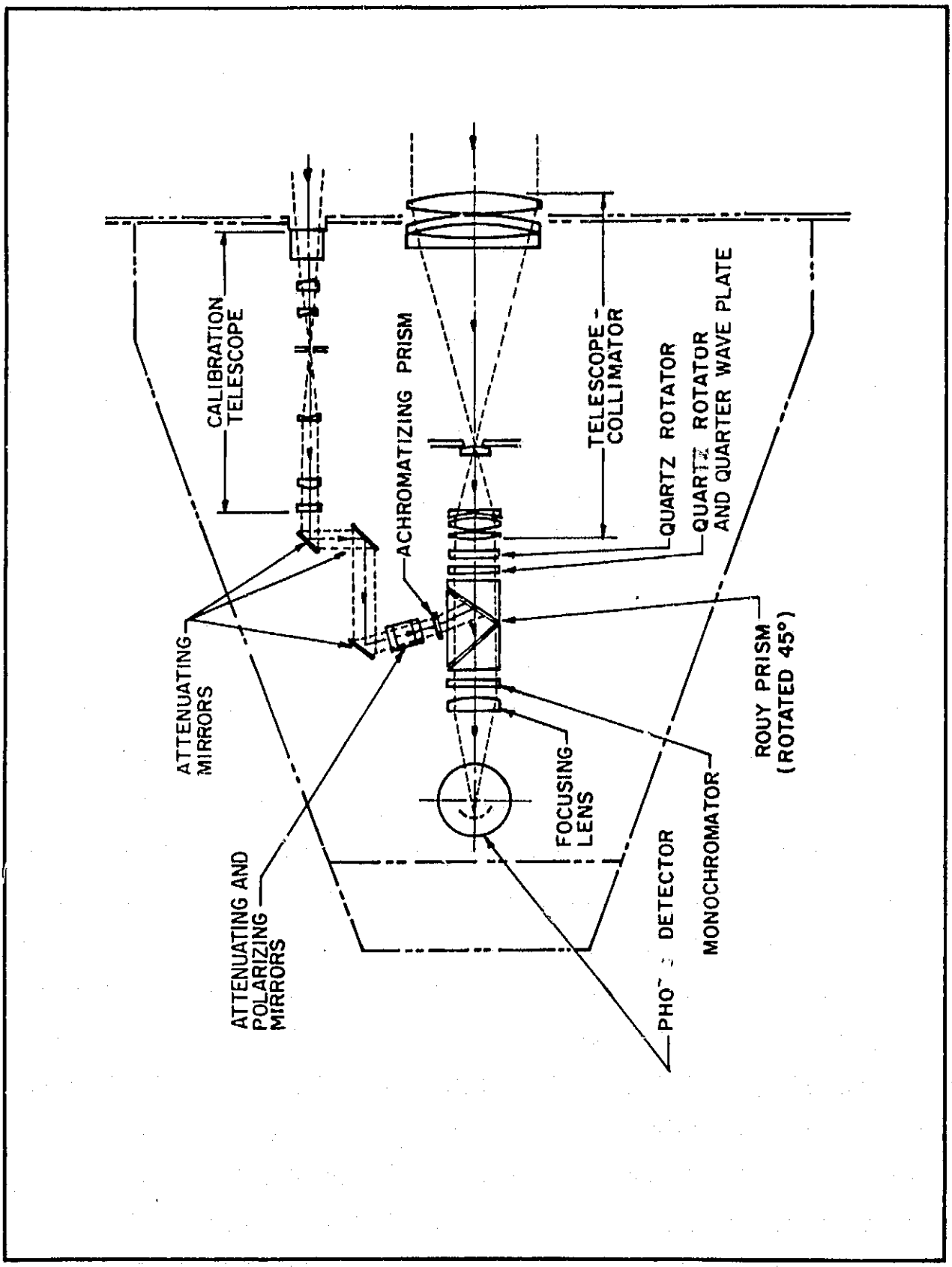

FIG. 2-1 Optical Layout

Bonn and Wolf show how the coherency matrix or the Stokes parameters may be used to describe the parameters of a partially polarized beam based on three sets of orthogonal intensity measurements but alas it appears that the authors assume that the Lord makes ideal optical elements; the above mentioned sources of extinction are not considered. A rigorous treatment was made by Battelle which will be given later, to incorporate these sources of extinction for the Rutgers instrument.

The Rutgers polarimeter contains two innovations. One is the Rouy double cut prism which when a set of these are crossed the intensity of a light beam is reduced by five to six orders of magnitude. The other innovation is that the analyzer (which is placed in front of the photomultiplier see figure 2.1) is not rotated to the settings of the various angles as in the conventional case but instead is kept in an invariant orientation with respect to the photomultiplier. This feature makes possible high accuracy. The reason is that mechanical rotation of the analyzer in front of the photomultiplier causes the transmitted beam to wander on the surface of the photosensitive element. The surface is not exactly uniform with the result that a serious source of error is introduced.

Instead of mechanically rotating the analyzer, the plane of polarization of the incoming beam is rotated by means of "right handed" and "left handed" quartz plates called rotators - the thickness of the rotators being determined by the wavelength of the filters. It should be noted however that this advantage is offset somewhat by the introduction of an additional element, the ellipticity

factor introduced by the rotators, since these elements possess optical activity. This factor is small and has been overlooked in all of the following treatments. However the factor can be determined and corrected for.

2.2 The Rouy Method

The Rutgers instrument is of a classic design and is capable of yielding values of high accuracy. Unlike the brightness measurements which may be obtained directly, polarization measurements require a more complicated combination of data and instrument parameters. The method of combining data and instrument parameters is somewhat controversial. In part this is due to the order of accuracy desired. To attempt to examine Dr. Rouy's method at this time has the elements of an inquest.

The Rouy equations appear to be contained in a BBRC Final Report of 1966. They are given as

$$2.1 \qquad R_1 = \frac{1/2\ A_o^2}{1/2\ A_o^2 + E_u} \qquad \text{where}$$

$$2.2 \qquad R_1 \equiv \frac{I_2 - I_1}{I_2 + I_1}$$

In addition

$$2.3 \qquad R_2 = \frac{1/2\ A_o^2}{1/2\ A_o^2 + E_u} \sin 2\theta \qquad \text{where}$$

$$2.4 \qquad R_2 \equiv \frac{I_4 - I_3}{I_4 + I_3}$$

Here I_i, $i = 1,2,3,4$, represent the intensity measurements for the corresponding positions as described in table 2.1 and $1/2\ A_o^2$ and E_u represent the energy of the polarized and unpolarized radiation respectively. Thus R_1 represents the degree of polarization in the Rouy method.

Taking

$$2.5 \qquad R_3 \equiv \frac{I_6 - I_5}{I_6 + I_5}$$

as the set of measurements given in equation 2.2 with the exception that a quarter wave plate has been inserted between the rotators and analyzer, the ellipticity i.e. the ratio of the minor to the major axis of the ellipse is given as

$$2.6 \qquad \frac{R_3}{R_1} = \frac{b}{a}$$

Though no account is taken of sources of extinction such as absorption, reflection and scattering it should be noted that each R value contains the same number of optical elements i.e. rotators, quarter wave plate and an invariant positioned analyzer with respect to the light transducer. Also the Rouy R values are of the form, $\frac{I_i - I_j}{I_i + I_j}$. Thus first (or perhaps zero) order approximation the transmission coefficient for a particular mode may be neglected.

The quarter wave plate was designed for the 5000 Å color filter. Appropriate corrections must be made for the 4000 and 6100 Å filters. Wave length corrections for the rotators are not required since these have the proper thicknesses for the 4000 and 6100 Å filters. However the nominal values were off as much as 2 degrees

in some cases and no provision for this effect was made in the Rouy equations.

Perhaps the most serious defect of the Rouy equations is that the plane of polarization of the zodiacal light is assumed to be coincident with the spin-axis of the vehicle. This is immediately apparent when it is realized that equation 2.1 or 2.2 contains no provision at all for this angle.

2.3 Donald Wilson Method

Dr. Wilson of BBRC collaborated with Dr. A. L. Rouy on various aspects of the Rutgers instrument for about four years. In the spring of 1970 shortly after the loss of Dr. Rouy, Dr. Wilson left BBRC. Some of his comments are contained here.

Dr. Wilson was aware of the inadequacy of the Rouy equations. In particular he was concerned with the fact that the rotators departed from their nominal values of $\pm 45^{\circ}$ by about 1 to 2 percent. A mean value γ_o for the apparent excursions of the pass-axes of the analyzer from the spin-axis was defined as

$$\gamma_o \equiv \frac{\gamma_1 + \gamma_2}{2}$$

$$\theta \equiv \frac{\gamma_2 - \gamma_1}{2}$$

The angles γ_3 and γ_4 were referenced to γ_o viz.

$$\gamma_3 \equiv (\gamma_o + \xi) + \theta'$$

$$\gamma_4 \equiv (\gamma_o - \xi) - \theta'$$

Here ξ represents the offset of the mean of γ_3, γ_4 from γ_o; θ' represents the excursion. Note that γ_i, (i = 1,2,3,4) represents the angle of the rotation for position "i". Further by defining α as

$$\alpha \equiv (\beta - \gamma_o)$$

where β is the fixed angle between the pass-axis of the analyzer and the spin-axis, R_2 is found as

$$2.7 \qquad R_2 = \frac{\sin 2\theta' \left(\sin^2 \alpha \cos 2\xi - \cos 2\alpha \sin 2\xi \right)}{\left[1 + \cos 2\theta' \left(\cos 2\alpha \cos 2\xi + \sin 2\alpha \sin 2\xi \right) \right] + \frac{2 E_u}{A_o^2}}$$

A somewhat more involved expression is found for R_1. The net result is that

$$2.8 \qquad \text{Cos } 2\alpha = \left(\frac{f_1 (R_1, R_2)^2}{R_1^2 + f_2 (R_2)^2 + f_1 (R_1, R_2)^2} \right)$$

The functions f_1 and f_2 are complicated trigonometric expressions containing the ratios of R_1 and R_2. A typical expression would be:

$$2.9 \quad \left\{ K_1^2 \cos^4\beta + 2K_1L_1 \cos^2\beta \ (1 - \cos^2\beta) + L_1^2 \ (1 - \cos^2\beta)^2 \right\}$$

$$- 2 \frac{R_1}{R_2} \left\{ K_1 \cos^2\beta + L_1 \ (1 - \cos^2\beta) \right\} \left\{ K_2 \cos^2\beta + L_2 \ (1 - \cos^2\beta) \right\}$$

$$+ \left(\frac{R_1}{R_2} \right)^2 \left\{ K_2^2 \cos^4\beta + 2K_2L_2 \cos^2\beta \ (1 - \cos^2\beta) + L_2^2 \ (1 - \cos^2\beta)^2 \right\}$$

$$= \left\{ M_1^2 - 2 \frac{R_1}{R_2} M_1M_2 + \left(\frac{R_1}{R_2} \right)^2 M_2^2 \right\} \cos^2\beta \ (1 - \cos^2\beta)$$

Additional equations of this type may be found in the Wilson BBRC (1970) report. In the author's opinion these expressions are of little utility other than pointing out the inadequacies of the original Rouy treatment.

2.4. The Battelle Study

The Battelle - Northwest Laboratories were called in briefly during 1971 to assist in various aspects of this project. One of these was an exact treatment of the experimental data to calculate the degree of polarization P and the angle Φ of polarization. Their expressions are given on the following pages as equations 2.10 and 2.11.

2.10 $$P = \left\{ \left[\frac{I_1-(I_2/I_2)}{I_1+(I_2/T_2)}\right]^2 + \left[\frac{(I_3/T_2)-I_4}{(I_3/T_2)+I_4}\right]^2 + \left[\frac{T_3}{T''}\left(\frac{I_5+(I_6/T_2)}{(I_3/T_2)+I_4}\right)-1\right]^2 \sin^{-2}\delta_i \right\}^{\frac{1}{2}}$$

2.11 $$\Phi = \arctan\left\{ \begin{matrix} P-\left[\frac{(I_3/T_2)-I_4}{(I_3/T_2)+I_4}\right] \\ \hline P+\left[\frac{(I_3/T_2)-I_4}{(I_3/T_2)+I_4}\right] \end{matrix} \right\}^{\frac{1}{2}} \left[\left(\frac{I_1-(I_2/T_2)}{I_1+(I_2/T_2)}\right)\left(\left[\frac{I_1-(I_2/T_2)}{I_1+(I_2/T_2)}\right]^2 + \left[\frac{T_3}{T''}\left(\frac{I_5+(I_6/T_2)}{(I_3/T_2)+I_4}\right)-1\right]^2 \sin^{-2}\delta_i\right)^{-\frac{1}{2}} \right.$$

$$\left. + \left[1 - \frac{T_3}{T''}\left(\frac{I_5+(I_6/T_2)}{(I_3/T_2)+I_4}\right)\right](\sin^{-1}\delta_i)\left(\left(\frac{I_1-(I_2T_2)}{I_1+(I_2/T_2)}\right)^2\left(\left[\frac{I_1-(I_2/T_2)}{I_1+(I_2/T_2)}\right]^2 + \left[\frac{T_3}{T''}\left(\frac{I_5+(I_6/T_2)}{(I_3/T_2)+I_4}\right)-1\right]^2 \sin^{-2}\delta_i \right)^{-\frac{1}{2}} \times \right.$$

$$\left. \frac{1}{2}\left(P - \left[\frac{(I_3/T_2)-I_4}{(I_3/T_2)+I_4}\right]\right) \sin\left[2 \arccos\left(\left(\frac{I_1-(I_2/T_2)}{I_1+(I_2/T_2)}\right)\left(\left[\frac{I_1-(I_2/T_2)}{I_1+(I_2/T_2)}\right]^2 + \left[\frac{T_3}{T''}\left(\frac{I_5+(I_6/T_2)}{(I_3/T_2)+I_4}\right)-1\right]^2 \sin^{-2}\delta_i\right)^{\frac{1}{2}}\right)\right] \times \right.$$

$$\left(\left[\frac{1}{4}\left(P + \left[\frac{(I_3T_2)-I_4}{(I_3/T_2)+I_4}\right]\right)^2 + \frac{1}{4}\left(P - \left[\frac{(I_3/T_2)-I_4}{(I_3/T_2)+I_4}\right]\right)^2 + \frac{1}{2}\left(P + \left[\frac{(I_3/T_2)-I_4}{(I_3/T_2)+I_4}\right]\right)\left(P - \left[\frac{(I_3/T_2)-I_4}{(I_3/T_2)+I_4}\right]\right)\cos\left[2 \arccos \right.\right.\right.$$

$$\left.\left.\left. \left(\left(\frac{I_1-(I_2T_2)}{I_1+(I_2/T_2)}\right)\left(\left[\frac{I_1-(I_2/T_2)}{I_1+(I_2/T_2)}\right]^2 + \left[\frac{T_3}{T''}\left(\frac{I_5+(I_6/T_2)}{(I_3/T_2)+I_4}\right)-1\right]^2 \sin^{-2}\delta_i\right)^{-\frac{1}{2}}\right]\right)^{\frac{1}{2}} + \right.$$

$$\left. \frac{1}{2}\left(P + \left[\frac{(I_3/T_2)-I_4}{(I_3/T_2)+I_4}\right]\right) + \frac{1}{2}\left(P - \left[\frac{(I_3/T_2)-I_4}{(I_3/T_2)+I_4}\right]\right)\cos\left[2 \arccos\right.\right.$$

$$\left(\left(\frac{I_1-(I_2/T_2)}{I_1+I_2/T_2)}\right)\left(\left[\frac{I_1-(I_2/T_2)}{I_1+(I_2/T_2)}\right]^2+\left[\frac{T_3}{T''}\left(\frac{I_5+(I_6/T_2)}{(I_3/I_2)+I_4}\right)-1\right]^2\sin^{-2}\delta_i\right)^{-\frac{1}{2}}\right)^{-1}\Bigg]\Bigg\}$$

where δ_i and the T's are different for the different wavelengths.

Clearly these equations are an achievement but in view of the lack of the parameters of the flight instrument their usefulness for the Rutgers experiment is questionable. However these equations reduce to simple forms when nominal values are used for the instrument parameters, these being essentially as follows:

2.12 $$R_1 = \frac{I_1 - I_2}{I_1 + I_2} \qquad R_2 = \frac{I_3 - I_4}{I_3 + I_4} \qquad R_3 = \frac{I_5 + I_6}{I_3 + I_4}$$

Polarization fraction:

2.13 $$P = \sqrt{R_1^2 + R_2^2 + (R_3 - 1)^2/\sin^2\delta}$$

$$A = \frac{1}{2}(1 - P)$$

$$B = \frac{1}{2}(R_2 + P)$$

$$C = \frac{1}{2}(-R_2 + P)$$

Relative phase:

$$\cos\xi = \frac{R_1}{\sqrt{R_1^2 + (R_3 - 1)^2/\sin^2\delta}}$$

$$\sin\xi = \frac{(1 - R_3)/\sin\delta}{\sqrt{R_1^2 + (R_3 - 1)^2/\sin^2\delta}}$$

ξ = relative phase of x and y component oscillations (see coherency matrix discussion for sign convention)

$$F = \frac{1}{2}\sqrt{B^2 + C^2 + 2BC\cos 2\xi}$$

Orientation of principle axis of polarized light oscillations:

2.14 $$\tan\phi = \sqrt{\frac{C}{B}}\left(\cos\xi + \sin\xi \frac{(C/2F)\sin 2\xi}{1 + (B/2F) + (C/2F)\cos 2\xi}\right)$$

The T values appearing in equations 2.10 and 2.11 are transmission coefficients and have been absorbed in the values for I_1 to I_6 that appear in equation 2.12. The phase change due to the introduction of the wave plate is δ. The utility of the nominal equations 33 and 34 will be discussed in section 2.6.

2.5 BBRC Final Report F70-11

A less exact treatment of the problem of evaluating the degree polarization and the angle of polarization, Φ appeared in this report. Using nominal values for the rotators and wave plate it was shown that

$$P = \sqrt{R_1^2 + R_2^2} \tag{2.15}$$

and

$$\Phi = 1/2 \tan^{-1} \frac{I_3 - I_4}{I_1 - I_2} \tag{2.16}$$

In the above expressions one assumes that the transmission factors for R_1 and R_2 are the same. However these expressions may be readily modified to include transmission factors. Expressions 2.15 and 2.16 have been used extensively in the present work.

2.6 Analysis of the Flight Instrument

Due to various circumstances a dry run on the flight instrument had not been carried out. Although the individual components of the Rutgers polarimeter were checked out, the assembled instrument was not tested before flight. As a result, for example, the shield to prevent stray light from entering the optical path of the polarimeter was subsequently found to be inadequate thus relegating the instrument

to the anti-solar direction, as the region for obtaining meaningful data for the zodiacal light. Though the prototype and copy of the instrument were subsequently examined the problem remained that the assembled flight instrument had not been tested as to the alignment and the nominal values of the optical elements, these including the rotators, the retarder and the fixed analyzer (Rouy prism). In a NASA Report by B. Carroll and F. E. Roach dated July 10, 1970 an analysis of the reliability of the flight instrument was made on the basis of the internal consistency of randomly selected quick-look data taken over orbits 200 to 4,600. The assessment of the flight instrument was considered from the following viewpoint.

The incident radiation may be given in terms of two components which may be selected as elliptically polarized and unpolarized radiation, linearly polarized radiation being taken as a special case of elliptical radiation. Since the rotators and quarter-wave plate should have no effect upon the unpolarized radiation other than possible absorption, reflection, and scattering the total radiation may be considered a super-position of the two components.

Any polarized beam regardless of the degree of ellipticity may be subdivided into two beams that are linearly polarized along any desired pair of mutually perpendicular directions. To each selected orthogonal set of axes there will correspond a phase difference, δ between the two components of the initial beam. The equation of the ellipse may be described as

2.17 $$\frac{E_x^2}{A_o^2} + \frac{E_y^2}{B_o^2} - \frac{2E_x E_y}{A_o B_o} = \sin^2 \delta$$

where E_x and E_y are the components of the electric vector and A_o and B_o are the corresponding amplitudes in the coordinate system x and y. When the ellipse is referred to its principal axes a_o and b_o using he coordinate system x^1 and y^1 then equation 2.17 becomes obviously

$$2.18 \qquad \frac{E_{x^1}^2}{a_o^2} + \frac{E_{y^1}^2}{b_o^2} = 1$$

The important relationship obtained from equations 2.17 and 2.18 is

$$2.19 \qquad a_o^2 + b_o^2 = A_o^2 + B_o^2$$

Since the squares of the amplitudes are proportional to the intensities equation permits one to state that the sum of the intensities for the three sets of orthogonal measurements for the Rutgers instrument should be equal i.e.

$$2.20 \qquad I_1 + I_2 = I_3 + I_4 = I_5 + I_6$$

Among the assumptions contained in equation 2.20 are

1. the transmission coefficients for the various modes (1-6) are equal
2. the nominal values for the rotators are such that the sets are orthogonal

In examining the quick-look data it was found that equation 2.20 held within an experimental error of $\pm$ 5%. The above treatment may be considered a zeroth order approximation. In view of the finding that equation 2.20 holds it will be seen that the Battelle equation 2.13 reduces to the BBRC equation 2.15. The latter was to use by our group in estimating the degree of polarization.

Further examination of the quick-look data showed that the fast axis of the quarter wave plate was at 45° to the optic axis of the Rouy prism. There had been some confusion regarding the orientation of the retarder. Apparently this arose because though the Rouy prism was fixed with its optic axis at 45° to the spin axis of the vehicle, the effective position (mode 1) of the optic axis was parallel (or perpendicular) to the spin-axis.

Additional aspects of the flight instrument are discussed in the following sections. In conclusion it should be noted that the absolute values of the polarization and $\bar{\Phi}$ may be uncertain within a few percent because of possible departures from the nominal values, nevertheless because of the stability of the Rutgers polarimeter the instrument becomes an effective differential probe of the zodiacal light.

3.0 INSTRUMENT PERFORMANCE

The Rutgers Zodiacal Light Analyzer experiment on OSO-6 was based on the scientific goals and requirements discussed in Sections 1 and 2. The success of the experiment is primarily a function of the instrument developed and its performance in orbit. In this section we present the major performance characteristics of the instrument.

3.1 INSTRUMENT DEVELOPMENT

The Zodiacal Light Analyzer instrument was conceived by the late Dr. T. Rouy, with scientific direction from Dr. B. Carroll, Rutgers, and Dr. L. Aller UCLA, under NASA Contract NAS5-9276 . The instrument was developed to the specifications and requirements established by Rutgers. This development effort was performed by Ball Brothers Research Corporation under Contract No. NAS5-9276/2.

The instrument is a photopolarimeter installed in one of the compartments of the rotating OSO wheel. It consists of a telescope, spectral filters, a Rouy prism, a detector and the necessary electronics to operate the various mechanisms and to handle the data produced. Table 3-1 gives the major characteristics of this instrument. The instrument is described in detail in the following reference documents:

(1) BBRC Report F70-11, "Rutgers Zodiacal Light Analyzer for OSO-6."

3.2 ORBITAL OPERATION

The OSO-6 was launched on August 9, 1969, and the ZLA instrument was put in operation soon after the start of orbital operations for the mission. The instrument was in continuous operation for

13626 orbits and was turned off at the end of the official mission on January 21, 1971. All functions of the instrument performed well throughout this period. The operational characteristics are discussed below.

3.2.1 Instrument Activation

The first activation activity for this instrument was the release of the extendable light baffle tube which was attached to the OSO compartment rim. This was restrained with pyrotechnically controlled devices which were fired by ground command. After firing, the spring-loaded baffle section was extended to its full open position and the protective aperture cover was ejected. This extension worked normally, and the instrument was successfully powered and placed into its automatic operation. The verification that the baffle section did extend to its full open position is based on the quality of the data obtained from the instrument, which were consistent with a fully opened baffle.

3.2.2 Operational Modes

The instrument was designed with various automatic and commandable modes of operation. The instrument took data every five degrees of elongation from the Sun, at three spectral filter settings and six polarization settings of the Rouy prism. A shutter blocking the optical path closed after every three elongation settings, and the instrument operated throughout an orbital day. A separate Sun calibration was obtained from a direct-viewing, auxiliary optical system once per orbital day.

The elongation angles from the Sun were measured by three solar detectors mounted 120 degrees apart around the wheel of the spacecraft. These established the 5-degrees-apart positions from the Sun and the logic of the instrument stepped through the 27 sequence

steps from -195 degrees through 0 to 195 degrees (three elongation angles were read at each logic position). Five data points were obtained for each setting of the Rouy prism, and then the spectral filter was stepped to a new setting. Each of these mode operations is discussed below.

3.2.2.1 Elongation Sensing and Sequencing

Each of the three solar sensing eyeblocks worked as designed and triggered the data taking every five degrees of elongation from the Sun to within about 1/2 degree. This has been verified by the identification of discrete stars in the data. The logic was designed to permit data taking in both directions around the celestial great circle described by the plane of the rotating wheel (the instrument optical axis was in this plane). This direction was established by ground command and was changed approximately 50 times throughout the mission. The sensing eyeblocks and the sequencing logic worked as designed throughout the mission and permitted repetitive measurements at known elongation angles from the Sun, independent of the spacecraft spin rate.

3.2.2.2 Rouy Prism and Spectral Filter Sequencing

The Rouy prism was designed to work with a series of quartz quarter-wave plates, which rotated in two wheels to place them in the optical beam. A third rotating wheel carried the spectral filters. These three wheels sequenced continuously throughout a pattern of 18 settings for each elongation setting. Five data points were taken at each setting and the logic directed the proper setting. Each of these three wheels operated as designed throughout the mission for a history of 6.6×10^6 individual stepping operations.

3.2.2.3 Shutter Sequencing

The optical system included a shutter to inhibit any direct sunlight from entering during each rotation. This shutter was opened by command from the elongation sensors and closed by logic following each triad of sky measurements. This mechanism operated successfully throughout the orbital lifetime for a history of 2.87 x 10^9 individual open/close operations.

3.2.2.4 Albedo Sensing

A separate albedo sensor was used to sense the direct sunlit Earth or the direct Sun to close the shutter and inhibit the normal sequencing. This sensing system operated correctly, shutting off the normal operation when the bright input levels were reached.

3.2.2.5 Direct Sunlight Calibration

An independent optical system was used to put direct sunlight through the system for calibration purposes. This beam was attenuated to approximately the same level as the zodiacal light and passed through the Rouy prism and filters. This subsystem worked corrected throughout the mission.

3.3 ORBITAL SENSITIVITY

The scientific data obtained from this experiment were based on the instrument sensitivity in orbit. Since the prelaunch calibrations were incomplete, the instrument sensitivity was determined from the orbital data.

3.3.1 Photometry

The photometric sensitivity in the three wavelength bands was determined by observation of known stars. A calibration was

established using a variety of stars from visual magnitude +6 to 0. In addition, the brightness of the gegenschein and Milky Way were correlated with this calibration, shown in Figure 3-1, for the 5000 Å band.

The 4000 Å and 6100 Å band sensitivities were related to this 5000 Å calibration by correlating the color indices of several known stars from these data, with the established color indices for them. These relative calibrations are:

$$B\text{-}V = 2.5 \log \frac{R_{4000}}{R_{5000}} - 0.7810$$

$$V\text{-}R = 2.5 \log \frac{R_{5000}}{R_{6100}} + 0.8940$$

$$B\text{-}R = 2.5 \log \frac{R_{4000}}{R_{6100}} + 1.6750$$

A similar correlation of the direct Sun calibration data has shown general agreement with these calibrations.

As with all photometric systems, the sensitivity degraded throughout the mission. The same stars and background were compared over the two years of coverage, and the following empirical relationship was determined for the degradation:

$$Count_T = Count_{Observed} \cdot e^{0.001T}$$

where T is the orbit number from the start of the mission. This degradation is expected for a space instrument and is about the normal amount.

The dark current for this instrument was approximately 100 counts. This was determined in obit, when the shutter was closed at the end of the orbit observing.

Figure 3-1

OSO-6 — RUTGERS Zodiacal Light Analyzer Experiment Calibration

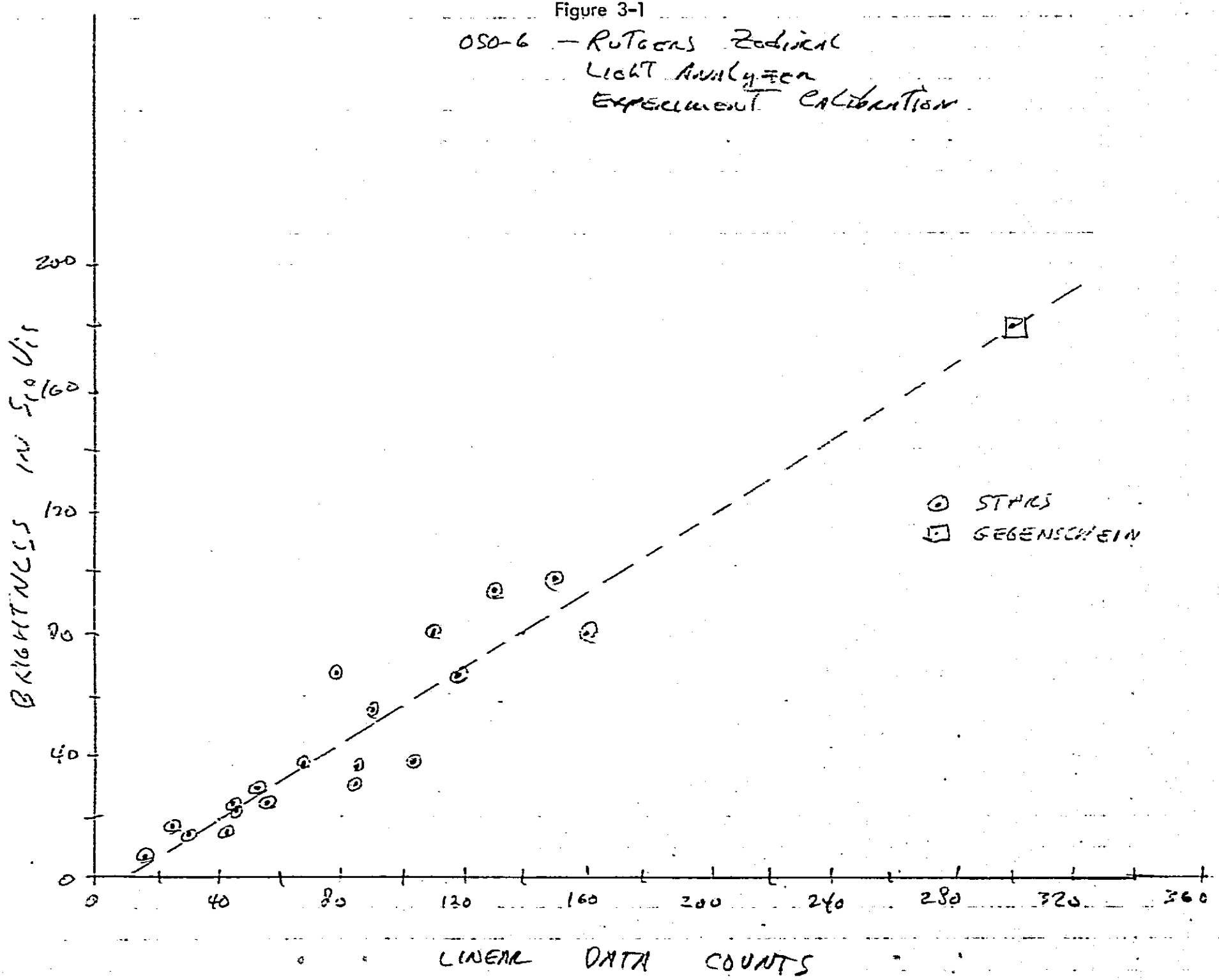

The instrument is affected by the influence of the South Atlantic Anomaly (SAA), as well as other anomalous zones around the earth. When the satellite is directly in the SMM, the count output increases to about 100 in the 4000 Å and 6100 Å data, and increases about 150 in the 5000 Å data. This is due to the direct interaction of energetic particles with the photomultiplier. The extra 50 counts at 5000 Å may be due to interaction between the particles and the optical filters, where the sensitivity is greater in the visible.

Normally the three color data obtained with this instrument were very stable, as seen in Figure 3-2, between the SAA peaks, where the average variation in the 4000 Å and 6100 Å data is about 5 counts; and in the 5000 Å, data is about 10 to 20 counts. The general decrease from orbit number 2380 to 2480 is due to the movement of the anti-Sun observation point above the Earth, from high latitudes to low latitudes. This 50-to-100 count variation is probably due to the effect of increased energetic particles activity at the higher latitudes, similar to the effect of the SAA.

We were able to discriminate +6.5 magnitude stars from the data taken in the anti-Sun direction, and in a cone of $\pm$15 degrees from the anti-Sun direction. Closer to the sun, the data were contaminated with scattered light from the sunlit Earth, and the data are unusable for measuring the sky background. We have also observed the moon on each lunation and have established an empirical calibration of the instrument sensitivity to scattered light. The amount of light entering the instrument is less than 0.1% of peak for angles greater than 7 degrees between the moon and the instrument line of sight. That is, any scattered light contribution from the moon is significantly less than gegenschein, at angles greater than 7 degrees, since no enhancement is seen in the gegenschein signal near the moon's electrometric signature.

Figure 3-2

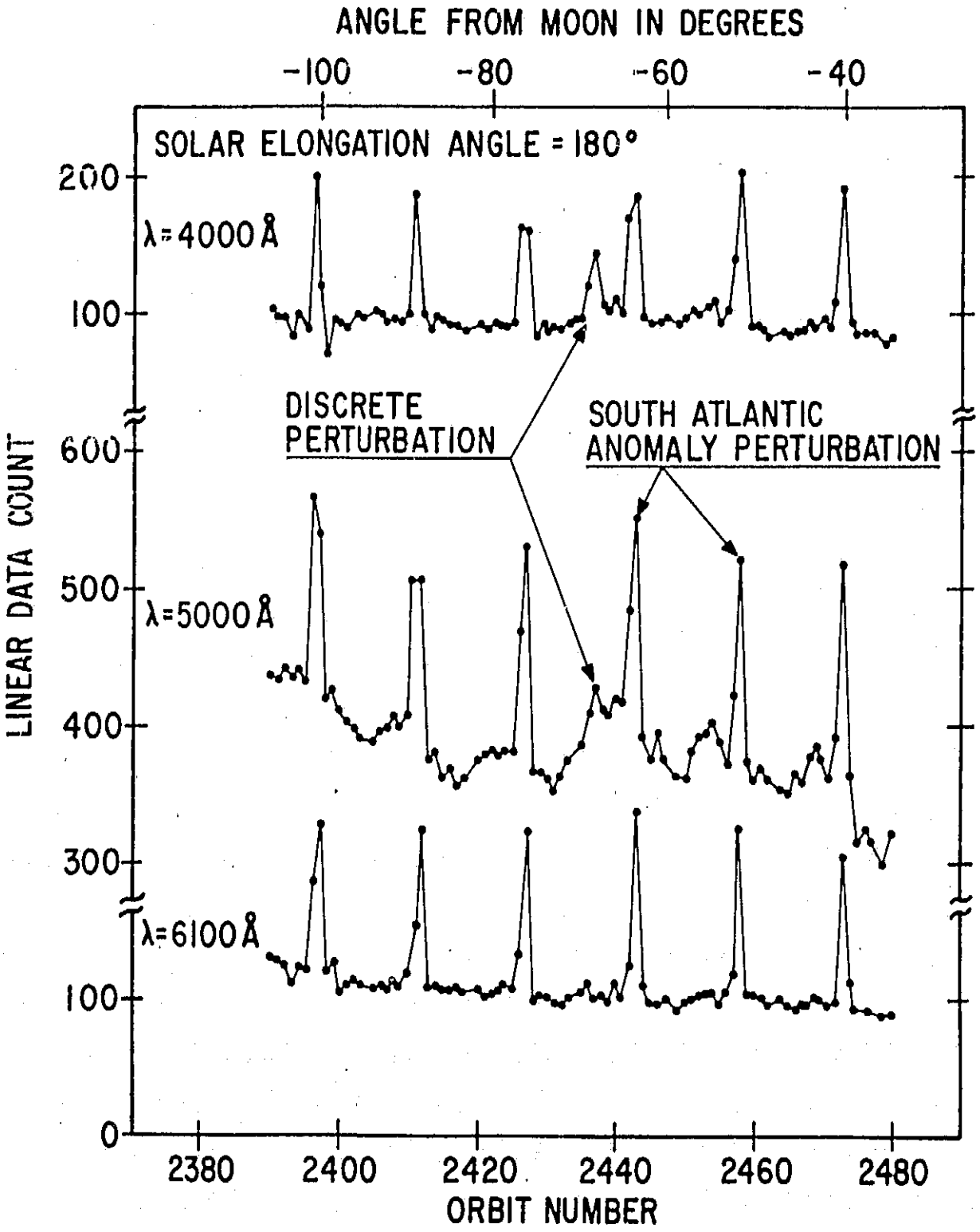
ANGLE FROM MOON IN DEGREES
-100
-80
-60
-40
SOLAR ELONGATION ANGLE = 180°
λ=4000 Å
λ=5000 Å
λ=6100 Å
DISCRETE PERTURBATION
SOUTH ATLANTIC ANOMALY PERTURBATION
LINEAR DATA COUNT
200
100
600
500
400
300
100
0
2380
2400
2420
2440
2460
2480
ORBIT NUMBER

Bright stars give a well-defined photometric signature. When tracked across the photocathode, they have given an empirical calibration of the cathode variations.

The photometric sensitivity of this instrument has been well established, with measurement probable errors of ±1 %. The color sensitivity has given good color temperature correlation data with known areas of the sky; e.g., solar temperature for the gegenschein and correlated temperatures for the Milky Way. This experiment has produced a wealth of photometric data and can be considered a major success.

3.3.2 Polarimetry

The linear and circular polarization sensitivity of this experiment has been extremely difficult to calibrate in orbit. However, using various smoothing techniques on the quiet, gegenschein sky background, we have established that the instrument has a linear polarization sensitivity of about ±0.5%. Therefore, this instrument is a high-quality polarimeter. Some circular polarization data have been analyzed, and significant results seem to be possible for strong signals.

DATA PROCESSING AND ANALYSIS

This section covers the evolution of the experiment data processing and the analytical approaches used to develop calibrations and useful scientific data.

4.1 Quick Look Data

The quick look data for the Rutgers Zodiacal Light Analyzer experiment was provided by NASA/GSFC throughout the OSO-6 mission, and they have been extensively used to provide early evaluation of the experiment performance. They have also been used to fill in specific details of sky coverage prior to the processing of the final data tapes. During the first few months of the mission we received quick look printouts of several complete orbits per day. This rate reduced to one complete orbit per day throughout the balance of the mission. These printouts were formulated to show each of the prime and housekeeping data words produced by the experiment. The printouts were produced by the OSO Control Center and a sample is shown in Fig. 4-1.

The data shown on these printouts are the decimal conversions of the telemetered prime data; presented by elongation angle from the sun, wavelength, and polarization setting. The housekeeping data are converted to engineering values based on calibrations developed during the final instrument checkout prior to launch.

The prime data were analyzed from these quick printouts initially to determine the basic instrument performance. From this analysis we determined the characteristics of the scattered light entering the instrument, and proceeded to evaluate the

FIG 4-1 QUICK LOOK PRINTOUT

E 71/12/12 RUTGERS STATE UNIVERSITY OSO-3 QUICK LOOK

MT	WHL3 λ	WH2 Polaniz setting	WH1	ANG1 ELONG ϕ	DATA1 DATA COUNT	ANG2	DATA2	ANG3	DATA3	ANG1	DATA1	ANG2	DATA2	ANG3	DATA3	D
502	CLSD	CAL	-45	0	0048	0	0053	0	0051	0	0048	0	0053	0	0051	
504	CLSD	CAL	-45	0	0044	0	0050	0	0047	0	0044	0	0050	0	0047	
506	CLSD	CAL	-45	0	0043	0	0044	0	0045	0	0043	0	0044	0	0045	
508	CLSD	CAL	-45	0	0039	0	0041	0	0040	0	0039	0	0041	0	0040	
510	CLSD		-45	+ 15	0041	+ 10	0037	+ 5	0038		0041		0037		0002	
511	4000	CLR	-45	+ 15	0881+	+ 10	0160+	+ 5	0704+	+ 15	0881+	+ 10	0160+	+ 5	0704+	
513	4000	CLR		+ 15	0782+	+ 10	0105+	+ 5	0695+	+ 15	0782+	+ 10	0105+	+ 5	0695+	MOT
515	4000	+45		+ 15	0830+	+ 10	0128+	+ 5	0696+	+ 15	0830+	+ 10	0128+	+ 5	0696+	
517	4000	+45	-45	+ 15	0842+	+ 10	0128+	+ 5	0695+	+ 15	0842+	+ 10	0128+	+ 5	0695+	
519	4000	1/4	-45	+ 15	0810+	+ 10	0113+	+ 5	0694+	+ 15	0810+	+ 10	0113+	+ 5	0694+	
521	4000	1/4		+ 15	0853+	+ 10	0147+	+ 5	0699+	+ 15	0853+	+ 10	0147+	+ 5	0699+	
523	5000	CLR	-45	+ 15	1012+	+ 10	0215+	+ 5	0738+	+ 15	1012+	+ 10	0215+	+ 5	0738+	
525	5000	CLR	+45	+ 15	0932+	+ 10	0185+	+ 5	0733+	+ 15	0932+	+ 10	0185+	+ 5	0733+	
527	5000	+45	+45	+ 15	0979+	+ 10	0202+	+ 5	0740+	+ 15	0979+	+ 10	0202+	+ 5	0740+	
528	5000	+45	-45	+ 15	0979+	+ 10	0203+	+ 5	0745+	+ 15	0979+	+ 10	0203+	+ 5	0745+	
530	5000	1/4	-45	+ 15	0978+	+ 10	0197+	+ 5	0739+	+ 15	0978+	+ 10	0197+	+ 5	0739+	
532	5000	1/4	+45	+ 15	0984+	+ 10	0202+	+ 5	0743+	+ 15	0984+	+ 10	0202+	+ 5	0743+	
534	6100	CLR	-45	+ 15	0899+	+ 10	0171+	+ 5	0694+		0899+		0171+		0694+	
536	6100	CLR	-45	+ 15	0803+	+ 10	0133+	+ 5	0698+		0803+		0133+		0002+	
538	6100	+45	-45	+ 15	0858+	+ 10	0150+	+ 5	0696+	+ 15	0858+	+ 10	0150+	+ 5	0696+	
540	6100	+45	-45	+ 15	0861+	+ 10	0148+	+ 5	0697+	+ 15	0861+	+ 10	0148+	+ 5	0697+	
542	6100	1/4	-45	+ 15	0869+	+ 10	0156+	+ 5	0696+	+ 15	0869+	+ 10	0156+	+ 5	0696+	
544	6100	1/4	-45	+ 30	0847+	+ 25	0151+	+ 20	0691+	+ 30	0847+	+ 25	0151+	+ 20	0691+	
545	4000	CLR	-45	+ 30	0763+	+ 25	0782+	+ 20	0873+	+ 30	0763+	+ 25	0782+	+ 20	0873+	
547	4000	CLR		+ 30	0647+	+ 25	0668+	+ 20	0746+	+ 30	0647+	+ 25	0668+	+ 20	0746+	
549	4000	+45		+ 30	0708+	+ 25	0724+	+ 20	0815+	+ 30	0708+	+ 25	0724+	+ 20	0815+	
551	4000	+45	-45	+ 30	0710+	+ 25	0727+	+ 20	0821+	+ 30	0710+	+ 25	0727+	+ 20	0821+	
553	4000	1/4	-45	+ 30	0674+	+ 25	0694+	+ 20	0786+	+ 30	0674+	+ 25	0694+	+ 20	0786+	
555	4000	1/4		+ 30	0730+	+ 25	0747+	+ 20	0841+	+ 30	0730+	+ 25	0747+	+ 20	0841+	
557	5000	CLR	-45	+ 30	0911+	+ 25	0928+	+ 20	1002+		0911+		0928+		1002+	
559	5000	CLR	+45	+ 30	0812+	+ 25	0835+	+ 20	0902+		0812+		0835+		0002+	5000
600	5000	+45	+45	+ 30	0869+	+ 25	0892+	+ 20	0963+	+ 30	0869+	+ 25	0892+	+ 20	0963+	
602	5000	+45	-45	+ 30	0868+	+ 25	0890+	+ 20	0964+	+ 30	0868+	+ 25	0890+	+ 20	0964+	
604	5000	1/4	-45	+ 30	0868+	+ 25	0889+	+ 20	0961+	+ 30	0868+	+ 25	0889+	+ 20	0961+	
606	5000	1/4	+45	+ 30	0873+	+ 25	0894+	+ 20	0966+	+ 30	0873+	+ 25	0894+	+ 20	0966+	
608	6100	CLR	-45	+ 30	0765+	+ 25	0793+	+ 20	0880+	+ 30	0765+	+ 25	0793+	+ 20	0880+	
610	6100	CLR	-45	+ 30	0632+	+ 25	0666+	+ 20	0753+	+ 30	0632+	+ 25	0666+	+ 20	0753+	
612	6100	+45	-45	+ 30	0714+	+ 25	0743+	+ 20	0834+	+ 30	0714+	+ 25	0743+	+ 20	0834+	
614	6100	+45	-45	+ 30	0713+	+ 25	0741+	+ 20	0834+	+ 30	0713+	+ 25	0741+	+ 20	0834+	R ON A
616	6100	1/4	-45	+ 30	0727+	+ 25	0755+	+ 20	0846+	+ 30	0727+	+ 25	0755+	+ 20	0846+	
618	CLSD			+ 45	0696+	+ 40	0725+	+ 35	0819+	+ 45	0696+	+ 40	0725+	+ 35	0819+	

FIG 4-1 QUICK LOOK PRINTOUT

GERS STATE UNIVERSITY OSO-3 QUICK LOOK TRACKING STATION GROS

DATA3	ANG1	DATA1	ANG2	DATA2	ANG3	DATA3							
0051	0	0048	0	0053	0	0051							
0047	0	0044	0	0050	0	0047							
0045	0	0043	0	0044	0	0045							
0040	0	0039	0	0041	0	0040							
0038		0041		0037		0002							
0704+	+ 15	0881+	+ 10	0160+	+ 5	0704+							
0695+	+ 15	0782+	+ 10	0105+	+ 5	0695+	MOTOR	17	026	+ 5V 050	.71	19.	22. 244
0696+	+ 15	0830+	+ 10	0128+	+ 5	0696+							
0695+	+ 15	0842+	+ 10	0128+	+ 5	0695+							
0694+	+ 15	0810+	+ 10	0113+	+ 5	0694+							
0699+	+ 15	0853+	+ 10	0147+	+ 5	0699+							
0738+	+ 15	1012+	+ 10	0215+	+ 5	0738+							
0733+	+ 15	0932+	+ 10	0185+	+ 5	0733+							
0740+	+ 15	0979+	+ 10	0202+	+ 5	0740+							
0745+	+ 15	0979+	+ 10	0203+	+ 5	0745+		022	+12V 099		.71	19.	22. 245
0739+	+ 15	0978+	+ 10	0197+	+ 5	0739+							
0743+	+ 15	0984+	+ 10	0202+	+ 5	0743+							
0694+		0899+		0171+		0694+							
0698+		0803+		0133+		0002+							
0696+	+ 15	0858+	+ 10	0150+	+ 5	0696+							
0697+	+ 15	0861+	+ 10	0148+	+ 5	0697+							
0696+	+ 15	0869+	+ 10	0156+	+ 5	0696+							
0691+	+ 30	0847+	+ 25	0151+	+ 20	0691+		021	-12V 146		.71	19.	22. 246
0873+	+ 30	0763+	+ 25	0782+	+ 20	0873+							
0746+	+ 30	0647+	+ 25	0668+	+ 20	0746+							
0815+	+ 30	0708+	+ 25	0724+	+ 20	0815+							
0821+	+ 30	0710+	+ 25	0727+	+ 20	0821+							
0786+	+ 30	0674+	+ 25	0694+	+ 20	0786+							
0841+	+ 30	0730+	+ 25	0747+	+ 20	0841+							
1002+		0911+		0928+		1002+							
0902+		0812+		0835+		0002+	5000+45-45		020	ERR 238	.71	19.	22. 247
0963+	+ 30	0869+	+ 25	0892+	+ 20	0963+							
0964+	+ 30	0868+	+ 25	0890+	+ 20	0964+							
0961+	+ 30	0868+	+ 25	0889+	+ 20	0961+							
0966+	+ 30	0873+	+ 25	0894+	+ 20	0965+							
0880+	+ 30	0765+	+ 25	0793+	+ 20	0880+							
0753+	+ 30	0632+	+ 25	0666+	+ 20	0753+							
0834+	+ 30	0714+	+ 25	0743+	+ 20	0834+							
0834+	+ 30	0713+	+ 25	0741+	+ 20	0834+	R ON AUTO	NO	018	+ 5V 049	.71	19.	23. 248
0846+	+ 30	0727+	+ 25	0755+	+ 20	0846+							
0819+	+ 45	0696+	+ 40	0725+									

only in the anti-sun direction. In this observing region we found usable data that were not contaminated by scattered light. Subsequently we evaluated these anti-sun observations using the quick look printouts, which led to confirmation that the experiment data were valid and correlatable with other ground based observations.

The quick look data were then analyzed to determine the proper conversion factors to be applied to the non linear data. From this analysis we developed the first calibration of the instrument sensitivity to temperature. Thus we committed to a series of processing steps using this conversion calibration.

The quick look printout data have proven to be a valuable aid in our data processing efforts, and continue to be used for checks of specific coverage, not yet available in processed form.

4.2 Final Data Inventory

We have received a complete library of final data from GSFC, covering the prime scientific data; the instrument housekeeping data; the history of commands sent to the instrument; and the spacecraft pointing and orbital history. These data are in the form of computer magnetic tapes, and have been used throughout our data processing efforts. The following sections present the detailed inventory of final data received.

4.2.1 Prime Scientific Data

We have received a complete set of prime data tapes from the start of the

mission, on 8-9-69, through the completion of the mission on 2-1-71. This complete data history is furnished on 287 tapes and covers 13,626 orbits. Included on these tapes are the data from the spacecraft housekeeping channel which contains the instrument housekeeping data.

4.2.2 Attitude/Orbit Data

We have received a complete set of spacecraft attitude and orbit parameter data from the start of the mission to its conclusion. This tape inventory includes 76 tapes.

4.2.3 Command Data

We have received a complete history of the commands sent to the instrument, covering the entire mission. This tape inventory includes 48 tapes.

4.3 Data Processing

We have performed extensive data processing using the final data provided by NASA/GSFC. Once we confirmed the basic characteristics of the experiment data from the quick look data, we followed a series of evolutionary data processing steps as shown in Fig. 4-2. These are discussed in the following sections.

4.3.1 First - A Generation Data

The first generation A of data processing was performed by operating on the final data tapes to convert the telemetered data to engineering values that could be more easily evaluated. This conversion consisted of shifting the digital value to

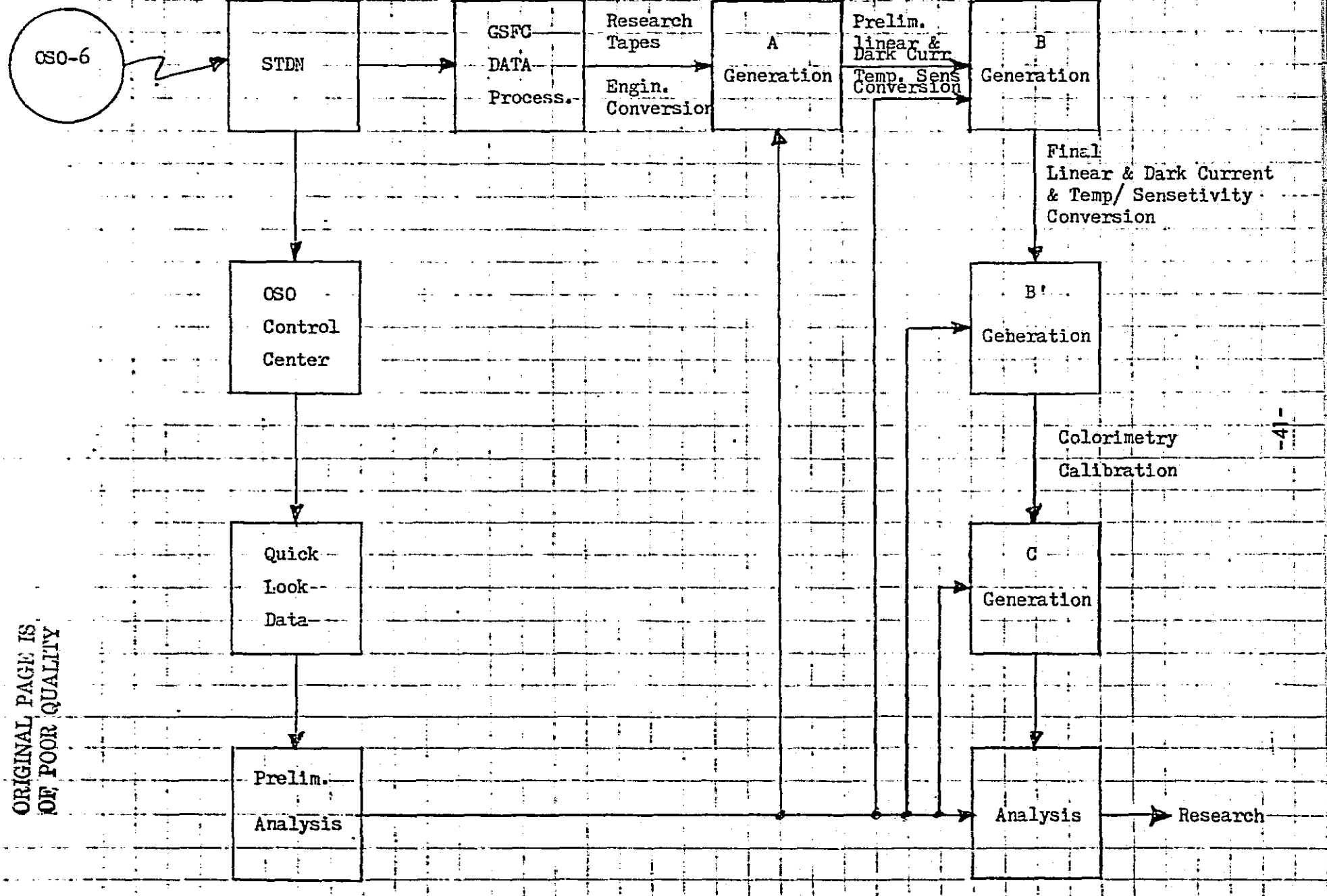

Figure 4-2 Rutgers Experiment Data Processing and Analysis Flow Diagram

correct a bias that the instrument inserted in the telemetered values. In addition to this conversion the data were formatted for printout according to wavelength and polarization for each elongation angle. A sample of the printout format is shown in Fig. 4.3.

The complete program used to generate this A generation of data was based on existing programs developed by BBRC during the checkout and integration of the ZLA in the OSO-6 prior to launch. Under a separate contract to Rutgers, BBRC added to this existing program, several calculations. These included averaging the five data points for each polarization setting; calculation of line of sight angles in the ecliptic, galactic and celestial coordinate systems, and to the earth's limb; OSO-6 ephemeris data; and decommutation of housekeeping data from the spacecraft commutator.

This program was used to process data from all elongation angles for the orbits indicated in Table 4-1. The A generation data were recorded on separate magnetic tapes and duplicate printouts were made of the six "anti-sun" elongation angles: 195, 190, 185, 180, 175, and 170 degrees, and 0 degrees, as well as several sets of dark current readings during the first part of satellite night.

4.3.2 Second - B Generation Data

The first or A generation data were used extensively to develop the empirical calibrations for the experiment. The major calibration developed was that to linearize the basic photometric data count, incorporating a correction for the dark current and the variation of count from the instrument as a function of

FIG. 4-3 A GENERATION PRINTOUT

ORBIT	DAY	MONTH	YEAR	PITCH	ROLL	SPI	RA SUN	DEC
6501	11	10	1970	.179	121.799	.512	196.353	-6

ELONGATION = -195

4000A						5000A						
-90	0	+45	-45	-90Q	0Q	-90	0	+45	-45	-90Q	0Q	-9
7777	159	7777	7777	7777	7777	7777	7777	7777	7777	7777	217	16
7777	169	7777	7777	7777	7777	7777	7777	7777	7777	7777	228	17
7777	169	7777	7777	7777	7777	7777	7777	7777	7777	7777	223	17
7777	151	7777	7777	7777	7777	7777	7777	7777	7777	7777	7777	16
7777	7777	7777	7777	7777	7777	7777	7777	7777	7777	7777	7777	16
AVERAGES												
7777	1685	7777	7777	7777	7777	7777	7777	7777	7777	7777	3244	17
LIMB ANGLES												
73.4	75.5	12.7	12.7	14.0	14.0	15.3	15.3	16.6	16.6	17.9	70.1	70.

MODE FLAG	EXP VIEW RA	EXP VIEW DEC	CEL VIEW RA	CEL VIEW DEC	GAL LONGITU
1.000	187.886	12.801	18.765	21.779	130.955
HUB TEMP	**DECK TEMP**	**DARK CURRENT**	**HUB VOLTAGE**	**DAY OF YEAR**	**TIME OF D**
105.500	105.500	30.000	237.000	284.000	10.968
OSO ALTITUDE	**X DOWN VECTOR**	**Y DOWN VECTOR**	**Z DOWN VECTOR**	**TARG LONGITUDE**	**TARG LATITU**
496.651	.629	-.430	-.648	50.377	21.779

ELONGATION = -190

4000A						5000A						
-90	0	+45	-45	-90Q	0Q	-90	0	+45	-45	-90Q	0Q	-9
7777	161	7777	7777	7777	7777	7777	7777	7777	7777	7777	233	17
7777	153	7777	7777	7777	7777	7777	7777	7777	7777	7777	231	17
7777	153	7777	7777	7777	7777	7777	7777	7777	7777	7777	224	16
7777	153	7777	7777	7777	7777	7777	7777	7777	7777	7777	7777	17
7777	7777	7777	7777	7777	7777	7777	7777	7777	7777	7777	7777	17

A GENERATION PRINTOUT

CH	ROLL	SPIN	RA SUN	DEC SUN	RA SP AX	DEC SP AX
79	121.799	.512	196.353	-6.960	105.027	-9.266

ELONGATION = -195

5000A						6100A					
-90	0	+45	-45	-90Q	0Q	-90	0	+45	-45	-90Q	0Q
7777	7777	7777	7777	7777	217	168	162	150	165	175	165
7777	7777	7777	7777	7777	228	174	158	164	166	155	171
7777	7777	7777	7777	7777	223	173	169	155	150	173	170
7777	7777	7777	7777	7777	7777	167	170	163	165	172	164
7777	7777	7777	7777	7777	7777	169	167	159	163	159	7777
AVERAGES											
7777	7777	7777	7777	7777	3244	170	165	158	162	167	1689
LIMB ANGLES											
15.3	15.3	16.6	16.6	17.9	70.1	70.1	70.1	69.0	69.0	67.9	67.9

CEL VIEW RA	CEL VIEW DEC	GAL LONGITUDE	GAL LATITUDE	RIM TEMP
18.765	21.779	130.955	-40.417	88.100
HUB VOLTAGE	DAY OF YEAR	TIME OF DAY	OSC LONGITUDE	OSC LATITUDE
237.000	284.000	10.968	-117.761	23.170
R Z DOWN VECTOR	TARG LONGITUDE	TARG LATITUDE	TARG ALTITUDE	CONE ANGLE
-.648	50.377	21.779	.298	68.087

ELONGATION = -190

5000A						6100A					
-90	0	+45	-45	-90Q	0Q	-90	0	+45	-45	-90Q	0Q
7777	7777	7777	7777	7777	233	179	174	174	170	161	153
7777	7777	7777	7777	7777	231	173	159	159	168	165	177
7777	7777	7777	7777	7777	224	165	161	162	161	163	178
7777	7777	7777	7777	7777	7777	170	173	166	164	176	156
7777	7777	7777	7777	7777	7777	170	166	160	158	166	7777

instrument temperature. (This characteristic of the instrument is described in Section 3). Using this empirical calibration the second or B generation data were produced. The B data processing was performed only on the six "anti-sun" elongation angles (195, 190, 186, 180, 175, and 170 deg.), and for both the observations near the satellite dawn and the repeat observations near satellite dusk.

The photometric calibration for conversion from the non-linear A generation data to the linear B data count has three main factors. Ths instrument design used a variable gain detection system, which exponentially factored the instrument output data count as a function of the detector output current. This calibration was not determined for the flight detector prior to launch, so the subsequent calibration of the flight spare detector was used as a first assumption. The second main calibration factor was the correction for the detector dark current. This was obtained by averaging the data taken by the normal operation of the instrument at the end of each satellite day, when the shutter was closed for night time. At this time a series of dark current readings were taken, and we have used these data to establish the necessary correction factor. The third main factor was the negative correlation of data count with instrument temperature. A temperature sensitive transistor in the electronics was flown, and its location was internal to the instrument assembly. We developed the empirical calibration of this effect as a function of the spacecraft hub temperature, which was the nearest, stable temperature monitor.

These three factors were combined into a preliminary calibration, which was used to generate the B generation data. We have used the linearized B data to determine the calibration for conversion to absolute units. The first step has been to use the many observed star crossings and calculating their color temperature, find the gain and temperature correction factor. This final algorythm was used to generate the B' data generation and is in the general form:

$$R = (Gd)_e^{-T} - DC$$

where: R is the final data count,

G is the detector gain inversely proportional to the high voltage,

d is the telemetered data count,

T is the electronics temperature.

The conversion from A to B to B' data was performed in two steps. The first was done by BBRC under contract to Rutgers, incorporating the preliminary calibration. The second was performed at Rutgers using the refined calibration based on analysis of the color temperatures of various stars observed. These two iterations were performed on the available A generation data for the orbits indicated in Table 4-1. Also included in the A to B conversion was the calculation of the grand average of the 30 readings per elongation per color.

A second major data processing step was also incorporated in the B generation data, to calculate the linear and circular polarization percentage and the projection of the electric vector on the celestial sky. This was calculated for

each set of readings and for the average of the five sets of readings per elongation angle per color.

An auxialliary data processing step was performed by BBRC for Rutgers, to plot the main data and the many pointing and housekeeping parameters. Duplicate sets of plots were produced for the main data count for each color for each of the six "anti-sun" elongation angles. Also duplicate plots were made of several of the key line of sight parameters.

The B and B' generations of data were presented in printout form. A sample of the B format is shown in Fig.4.4. These data have been used extensively for analysis and have led to the main scientific results from this experiment. In addition several auxilliary printouts were made by Rutgers from the B generation data for the six elongations:

RPO - 1 Four data count values for the linear polarization readings per color and their means; and housekeeping data;

RPO - 2 Six readings per color and their means;

RPO - 3 Means of readings per color and housekeeping;

RPO - 4 Line of sight angles;

4.3.3 Third - C Generation Data

Using the calibration determined from the two stage B generation data, we processed a third or C generation of data. This generation calculates the color indices and related sky temperatures from the calibrated three color data. Three color indices were calculated:

FIG 4-4 B GENERATION PRINTOUT

ORBIT	DAY	MONTH	YEAR	PITCH	ROLL	SPIN	RA SU
4748	18	6	1970	.249	108.699	.517	86.52

ORBIT NO. = 4748 ELONGATION = -195

4000A						5000A					
-90	0	+45	-45	-900	00	-90	0	+45	-45	-900	00
245	225	235	234	234	235	293	295	300	298	296	280
232	240	232	239	230	225	297	302	297	295	295	290
239	236	233	227	227	239	311	296	303	289	290	295
230	239	225	235	238	239	310	302	294	293	296	289
234	231	231	232	237	232	296	287	297	300	293	305
AVERAGES											
236.	234.	231.	233.	233.	234.	301.	296.	298.	295.	294.	292.
LIMB ANGLES											
76.2	75.6	75.1	74.6	74.2	73.7	73.2	72.8	72.3	71.8	71.3	70.9

MODE FLAG	EXP VIEW RA	EXP VIEW DEC	CEL VIEW RA	CEL VIEW DEC	GA
1.000	184.674	14.270	271.463	-9.164	

HUB TEMP	DECK TEMP	DARK CURRENT	HIGH VOLTAGE	DAY OF YEAR
7.710	82.100	51.000	236.000	169.000

OSO ALTITUDE	X DOWN VECTOR	Y DOWN VECTOR	Z DOWN VECTOR	TARG LONGITUDE	TA
500.501	.718	-.095	-.689	1.444	

4000A						5000A					
-90	0	+45	-45	-900	00	-90	0	+45	-45	-900	00
227	166	195	192	192	195	414	423	447	437	428	357
186	211	186	207	180	166	432	456	432	423	423	400
207	198	189	172	172	207	502	418	461	396	400	423
180	207	166	195	204	207	497	456	418	414	428	396
192	183	183	186	201	186	428	387	432	447	414	471
AVERAGES											
[illegible]		190.	190.	192.		455.	428.	438.	423.	419.	410.

ANG(I)	P(I)	P56	ANG(I)	P(I)	P56
2.89	15.52	-.78	-44.54	1.55	8.99
41.30	8.22	4.15	-22.03	2.92	2.77
64.83	5.38	-9.48	40.08	11.89	-2.77
49.09	10.73	-.76	7.42	4.28	3.88
-18.58	2.52	3.91	-18.05	5.26	-6.50

XBAR= -51.64 PB= 2.25 PB56= -.66 XBAR= 30.23 PB= 3.45 PB56= 1.09

AVERAGE DIGITAL COUNTS = 191. 429.

FIG 4-4 B GENERATION PRINTOUT

PITCH	ROLL	SPIN	RA SUN	DEC SUN	RA SP AX	DEC SP AX
.249	108.699	.517	86.530	23.404	4.552	-18.469

48 ELONGATION = -195

	5000A						6100A					
	-90	0	+45	-45	-900	00	-90	0	+45	-45	-900	00
	293	295	300	298	296	280	234	251	234	247	234	248
	297	302	297	295	295	290	245	243	248	243	243	242
	311	296	303	289	290	295	240	244	245	248	230	240
	310	302	294	293	296	289	245	244	236	239	243	241
	296	287	297	300	293	305	240	249	241	225	243	233
	AVERAGES											
.	301.	296.	298.	295.	294.	292.	241.	246.	241.	240.	239.	241.
	LIMB ANGLES											
	73.2	72.8	72.3	71.8	71.3	70.9	70.3	69.9	69.4	68.9	68.4	67.9

IEW DEC	CEL VIEW RA	CEL VIEW DEC	GAL LONGITUDE	GAL LATITUDE	RIM TEMP
.270	271.463	-9.164	19.857	5.205	63.300

CURRENT	HIGH VOLTAGE	DAY OF YEAR	TIME OF DAY	OSO LONGITUDE	OSO LATITUDE
.000	236.000	169.000	3.310	-1.053	-24.911

N VECTOR	Z DOWN VECTOR	TARG LONGITUDE	TARG LATITUDE	TARG ALTITUDE	CONE ANGLE
.095	-.689	1.444	-9.164	-.986	68.008

	5000A						6100A					
	-90	0	+45	-45	-900	00	-90	0	+45	-45	-900	00
6	414	423	447	437	428	357	192	247	192	233	192	237
6	432	456	432	423	423	400	227	220	237	220	220	217
7	502	418	461	396	400	423	211	223	227	237	180	211
7	497	456	418	414	428	396	227	223	198	207	220	214
6	428	387	432	447	414	471	211	240	214	166	220	189
	AVERAGES											
2.	455.	428.	438.	423.	419.	410.	213.	231.	212.	213.		

ANG(I)	P(I)	P56	ANG(I)	P(I)	P56
-44.54	1.55	8.99	37.85	15.77	-10.38
-22.03	2.92	2.77	67.98	3.88	.74
40.08	11.89	-2.77	35.99	3.65	-7.78
7.42	4.28	3.88	-72.44	2.40	1.48
-18.05	5.26	-6.50	-62.71	14.21	7.59

66 XBAR= 30.23 PB= 3.45 PB56= 1.09 XBAR= -2.72 PB= 3.92 PB56= -1.63

. 429. 215.

(1) B-V, the ratio of the 4000A data to the 5000A data;

(2) V-R, the ratio of the 5000A data to the 6100A data;

(3) B-R, the ratio of the 4000A data to the 6100A data;

The ratios were obtained from the average B' value of the 30 readings for each color, and for each of the six elongations.

The effective sky temperature was calculated based on a black body characteristic assumed for the group of stars used for calibration. This color temperature calibration is shown in Fig. 4-5 for the three indices. The effective sky temperature was calculated separately for each index and for the average of the indices. These data were presented both on magnetic tape and in two different printouts made by Rutgers:

RPO - 5 Initial color indices;

RPO - 10 Final color indices and color temperatures;

A sample of the RPO - 10 printout is shown in Fig. 4-6.

4.3.4 Log of Processed Data

The several generations of processed data were made for 57% of the orbits available, and are tabulated in Table 4-1. The final photometric data were processed only for the six "anti-sun" elongation angles for 54% of the available orbits or 10% of the total available sky readings.

Figure 4-5

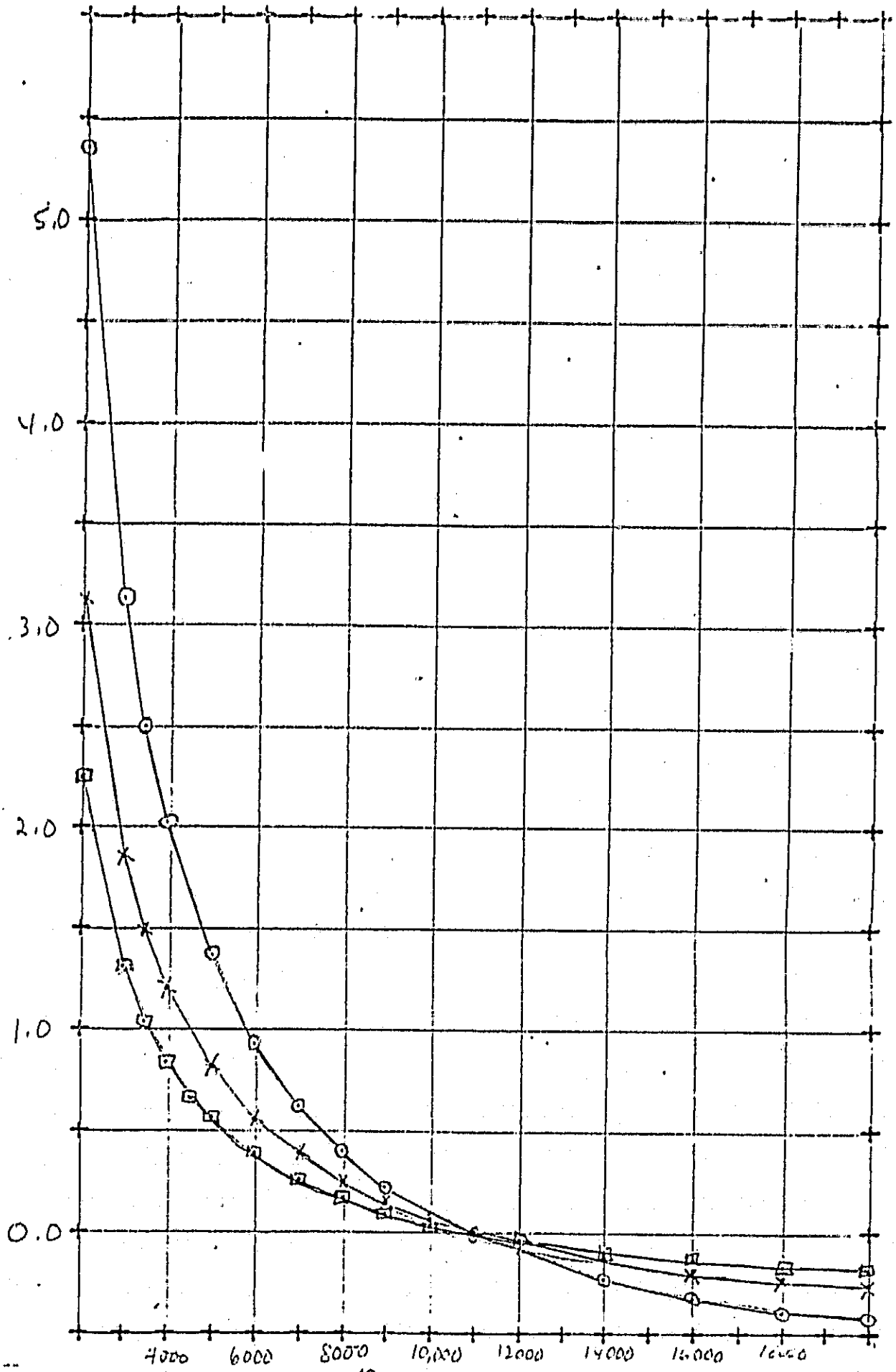
5.0
4.0
3.0
2.0
1.0
0.0
COLOR INDEX
4000
6000
8000
10,000
12000
14000
16,000

TABLE 4-1

LOG OF PROCESSED DATA

Orbit Sequence	No. of Orbits	Generation A	B	B'	C
584 to 7637	7053	X	X	X	X
8418 to 8511	93	X	X	-	-
9144 to 9319	175	X	X	-	-
10915 to 11074	159	X	X	-	-
11835 to 12111	276	X	X	X	X
13242 to 13257	15	X	X	-	-
Total:	7771				

4.3.5 Special Processing

Several special processing operations have been performed on the experiment data. These include smoother polarization percentage and angle calculations, plotting routines, background subtraction and isophotal contouring. These have been performed on the personal computers of two of the co-investigators, (FER and JRR), and have been an important factor in providing data for analysis. Other computer processing programs are being prepared by LHA, to correlate polarization characteristics with the interplanetary magnetic field characteristics.

4.4 ANALYSIS

The significant scientific results obtained from this experiment are from the analysis of the data processed. Throughout the data processing evolution, we

FOLDOUT FRAME 1

FIG. 4-6 C. GENERATION PRINTOUT

ELONGATION = -170 C1 = -0.7810 C2 = 0.8940 C3 = 1.67

ORBIT	DAY	TIME	D45	D55	D65	DC1	R45	R55	R65	B-V
584	259.	19.916	210.8	302.9	225.0	152.0	145.2	524.6	191.1	0.613
585	259.	21.490	210.9	300.2	224.9	189.2	116.1	491.3	163.3	0.785
586	259.	23.080	212.3	300.3	221.4	189.2	120.8	491.9	151.2	0.743
588	260.	2.250	214.1	247.8	224.9	189.2	126.6	248.5	163.2	-0.049
591	260.	5.419	212.4	294.3	216.2	189.2	120.9	459.8	133.8	0.669
592	260.	7.001	209.3	292.1	219.6	189.2	110.8	446.6	145.1	0.737
593	260.	8.583	213.6	289.6	217.2	189.2	125.0	435.9	136.9	0.575
594	260.	10.171	208.2	289.0	216.2	189.2	107.3	432.5	133.8	0.733
595	260.	11.724	34.5	0.0	0.0	152.0	-117.6	-152.0	-152.0	-0.502
595	260.	13.335	200.5	288.9	210.1	152.0	113.9	452.4	143.1	0.717
596	260.	14.923	201.2	285.9	212.6	152.0	116.0	437.4	150.8	0.660
597	260.	16.505	197.1	284.6	206.6	121.0	130.2	448.3	157.4	0.561
598	260.	18.087	192.7	282.1	203.0	121.0	118.3	436.9	146.9	0.637
599	260.	19.675	191.8	284.2	203.0	121.0	115.9	446.7	146.9	0.684
600	260.	21.257	198.5	286.2	208.2	152.0	108.0	438.8	137.1	0.741
601	260.	22.839	196.9	285.7	208.7	121.0	129.9	453.6	163.7	0.577
602	261.	0.427	202.3	287.2	212.8	152.0	119.4	444.0	151.4	0.645
603	261.	2.009	168.6	288.2	213.8	152.0	26.7	448.7	154.8	2.281
606	261.	5.179	199.0	286.5	210.0	152.0	109.5	440.3	142.7	0.730
607	261.	6.761	205.8	284.9	213.2	152.0	129.9	432.9	152.9	0.526
608	261.	8.343	207.1	287.9	214.8	152.0	133.7	447.3	158.0	0.530
609	261.	9.931	206.7	288.1	213.1	152.0	132.7	448.1	152.4	0.540
609	261.	11.472	70.2	0.0	0.0	152.0	-81.8	-152.0	-152.0	-0.108
610	261.	11.513	34.5	0.0	105.6	152.0	-117.5	-152.0	-46.4	-0.501
610	261.	13.095	200.7	286.6	210.3	152.0	114.6	441.1	143.6	0.683
611	261.	14.663	209.9	291.7	215.2	152.0	142.3	466.4	159.1	0.507
612	261.	16.265	208.0	289.9	218.3	152.0	136.7	457.2	169.0	0.530
613	261.	17.847	204.3	290.0	212.0	152.0	125.3	457.7	149.1	0.625
614	261.	19.435	206.1	291.5	213.9	152.0	130.7	465.0	155.1	0.597
615	261.	21.017	207.0	291.2	215.9	189.2	103.6	443.8	132.5	0.798
616	261.	22.599	210.5	293.8	213.9	152.0	144.4	477.0	155.1	0.516
617	262.	0.187	211.9	296.0	219.0	189.2	119.4	468.6	143.2	0.703
619	262.	3.351	213.4	294.8	221.7	189.2	124.2	462.4	152.3	0.646
622	262.	6.521	215.7	293.9	224.0	189.2	132.0	457.9	160.3	0.570
623	262.	8.103	220.7	295.4	225.7	189.2	148.7	465.6	166.2	0.458
624	262.	9.691	215.8	291.5	224.0	189.2	132.4	445.2	160.4	0.536
624	262.	11.273	212.0	291.3	218.0	189.2	119.6	444.5	139.8	0.644
625	262.	12.855	207.1	286.4	212.4	189.2	103.8	419.8	121.1	0.737
626	262.	14.443	209.9	287.8	215.7	189.2	113.0	426.6	131.9	0.662
627	262.	16.025	203.1	286.4	212.1	189.2	91.3	419.7	119.9	0.875
628	262.	17.607	195.6	282.3	200.3	152.0	99.6	420.1	113.5	0.782

C. GENERATION PRINTOUT

-0.7810 C2 = 0.8940 C3 = 1.6750

	DC1	R45	R55	R65	B-V	B-R	V-R	T21	T22	T23	T24	MODE
0	152.0	145.2	524.6	191.1	0.613	1.192	0.579	5704	5349	4933	5328	
9	189.2	116.1	491.3	163.3	0.785	1.264	0.479	5066	5200	5399	5221	
4	189.2	120.8	491.9	151.2	0.743	1.137	0.394	5204	5469	5898	5523	
9	189.2	126.5	248.5	163.2	-0.049	1.170	1.219	10935	5396	1841	6057	
2	189.2	120.9	459.8	133.8	0.669	1.003	0.334	5475	5794	6324	5864	
6	189.2	110.8	446.6	145.1	0.737	1.187	0.449	5226	5360	5559	5381	
2	189.2	125.0	435.9	136.9	0.575	0.993	0.417	5873	5822	5749	5814	
2	189.2	107.3	432.5	133.8	0.733	1.133	0.401	5241	5477	5853	5523	
0	152.0	-117.6	-152.0	-152.0	-0.502	1.173	1.675	18691	5389	-5456	6208	
1	152.0	113.9	452.4	143.1	0.717	1.142	0.425	5298	5459	5702	5486	
6	152.0	116.0	437.4	150.8	0.660	1.179	0.519	5510	5376	5200	5362	
6	121.0	130.2	448.3	157.4	0.561	1.100	0.539	5938	5555	5106	5533	
0	121.0	118.3	436.9	146.9	0.637	1.129	0.492	5603	5488	5333	5474	
0	121.0	115.9	446.7	146.9	0.684	1.151	0.467	5418	5437	5459	5438	
2	152.0	108.0	438.8	137.1	0.741	1.153	0.412	5212	5434	5784	5476	
7	121.0	129.9	453.6	163.7	0.577	1.145	0.568	5864	5450	4976	5430	
8	152.0	119.4	444.0	151.4	0.645	1.152	0.507	5570	5435	5256	5420	
8	152.0	26.7	448.7	154.8	2.281	2.800	0.519	-2557	2482	5197	1707	
0	152.0	109.5	440.3	142.7	0.730	1.182	0.452	5250	5370	5544	5388	
2	152.0	129.9	432.9	152.9	0.526	1.071	0.545	6108	5623	5078	5603	
8	152.0	133.7	447.3	158.0	0.530	1.075	0.545	6089	5615	5079	5594	
1	152.0	132.7	448.1	152.4	0.540	1.045	0.504	6038	5689	5269	5665	
0	152.0	-81.8	-152.0	-152.0	-0.108	1.567	1.675	11716	4673	-5456	3644	
6	152.0	-117.5	-152.0	-46.4	-0.501	-0.115	0.386	18676	11206	5948	11943	
3	152.0	114.6	441.1	143.6	0.683	1.139	0.456	5424	5465	5520	5469	
2	152.0	142.3	466.4	159.1	0.507	1.015	0.508	6203	5764	5253	5740	
3	152.0	136.7	457.2	169.0	0.530	1.124	0.594	6089	5498	4869	5485	
0	152.0	125.3	457.7	149.1	0.625	1.083	0.457	5652	5596	5515	5587	
9	152.0	130.7	465.0	155.1	0.597	1.080	0.483	5774	5602	5370	5584	
9	189.2	103.6	443.8	132.5	0.798	1.161	0.363	5024	5416	6113	5517	
9	152.0	144.4	477.0	155.1	0.516	0.971	0.455	6158	5878	5527	5854	
0	189.2	119.4	468.6	143.2	0.703	1.091	0.388	5346	5575	5939	5620	
7	189.2	124.2	462.4	152.3	0.646	1.115	0.469	5567	5519	5451	5512	
0	189.2	132.0	457.9	160.3	0.570	1.105	0.535	5897	5543	5123	5521	
7	189.2	148.7	465.6	166.2	0.458	1.014	0.557	6472	5765	5027	5754	
0	189.2	132.4	445.2	160.4	0.536	1.102	0.567	6061	5550	4984	5531	
0	189.2	119.6	444.5	139.8	0.644	1.063	0.419	5574	5642	5738	5651	
4	189.2	103.8	419.8	121.1	0.737	1.062	0.326	5228	5645	6391	5754	
7	189.2	113.0	426.6	131.9	0.662	1.062	0.400	5505	5646	5858	5669	
1	189.2	91.3	419.7	119.9	0.875	1.190	0.315	4795	5352	6475	5540	
3	152.0	99.6	420.1	113.5	0.782	1.036	0.254	5076	5710	7016	5934	
2	152.0	95.7	411.1	114.4	0.862	1.107	0.304	5011	5530	6545	5721	

have gained a deep insight into the significance, precision and accuracy of the experiment data. This insight has been used to iterate from first generation data to analysis and back to improved data generations. This has been essential to develop empirical calibrations and to isolate the useful data and the environmental variations in the data values.

This analysis has been performed by the usual techniques of hand plots and determination of correlation functions. We have made extensive cross correlations between the prime data and various instrumental and environmental effects. We have identified a library of stars in the data down to 6th magnitude. We have performed many trial analytical approaches with our personal mini-computers to ascertain the most fruitful lines of research. The main analytical approach has been to isolate features by their geometric or temporal characteristics, and the various scientific papers published indicates the productivity of our data processing and analysis techniques.

SCIENTIFIC RESULTS

5.1 INTRODUCTION

The initial phase of the investigations was centered on an evaluation of the quality of the data. As the program was conceived the plan was to make 5256 individual photometric readings of the sky during each satellite orbit. The program was active over a period of about two and a half years, almost 14,000 orbits. Thus, the reservoir of digitized readings included more than 80 million sky observations. The observations included the following elongations from the sun: -195° (5° steps) to -5°; $+5^{\circ}$ (5° steps) to $+195^{\circ}$. Calibration readings were also made during each orbit on the sun itself through special optics which attenuated the solar brightness to a level similar to the readings of the sky. The convention we have used is that a negative elongation refers to "morning" observations from the satellite's emergence from the Earth's shadow to "noon" and the positive elongations refer to the afternoon observations.

At each elongation, readings were made through filters centered at wave-lengths: 4000A, 5000A, and 6100A. For each color filter six polarizing elements were introduced into the optical path in such a way as to make possible the determination of the four Stokes parameters. Thus, the potential of a given orbit is the polarization in three colors at 76 elongations from the sun.

5.2 REJECTION OF SCATTERED LIGHT

The prime problem in observing the astronomical sky from a satellite which is above the surface daytime "sky" whose intensity prohibits such observations from the ground is the rejection of scattered light from bright objects in the sky, especially the sun. In Table 5-1 and figures 5-1 and 5-2 we show data and plots of the scattered light which reaches the photo surface based primarily on observations of the scattering of lunar light. It is noted that a bright object such as the moon contributes about 0.1% of its brightness due to scattered light into the optical system at an elongation

angle of 13 degrees. Since the moon moves in its orbit as seen from the Earth about 13 degrees per day the observations lost because of scattered moonlight occurred during a small fraction of each lunation.

The scattered sunlight is a much more serious problem since the sun is some 465,000 times as bright as the full moon. Thus, at an elongation of 13 degrees the scattered light from the sun is intolerably large. Even at elongations of 60 degrees to 90 degrees the observations with the Rutgers Photometer indicate that the scattered light from the sun, though reduced 10 (-10) of the brightness of the sun itself, is still too high to permit photometric observations with acceptable accuracy. This is evident from the fact that the level of brightness of the astronomical sky is of the order of 10 (-13) times the surface brightness of the sun. Thus, the instrumental scattered light is some 3 orders of magnitude greater than the brightness of the astronomical sky. The entire hemisphere of observations within 90 degrees of the sun is not available for analysis.

The antisun hemisphere leaves us with a residual of some 40 million observations. We have scanned this reservoir with the following conclusions:

(1) A significant fraction is seriously affected by the fact that the sunlit Earth is within the 90 degree rejection cone.

(2) A large fraction of the observations within what we may call the gegenschein cone (within 15 degrees of the antisolar direction) is not seriously affected by scattered light from either the sun or the sunlit Earth.

The main thrust of our research efforts has concentrated on this gegenschein cone although there is probably a significant amount of usable data outside this cone which we were not able to explore definitively.

5.3 THE PHOTOMETRIC DATA

The output of the research may be divided into three domains: (1) photometry, (2) colorimetry, (3) polarimetry. We propose to dis-

cuss these seriatim.

The fundamental precision of the photometric system is extraordinarily good as illustrated by Table 5-2 and Figures 5-3, 5-4, 5-5, 5-6, 5-7. An explanation of the significance of paired observations (negative and positive elongations) is given in Figure 5-3. We note that the individual elongations are carefully referred to the sun. In the interval of a half orbit, from extreme elongations of -195 degrees to +195 degrees, the sun's apparent motion along the celestial sphere background is about 0.03 degree compared with the field of view of our photometer of 2 degrees. Within the small uncertainty of this effect the paired observations: -180°, $+180^{\circ}$; -175°, $+185^{\circ}$; -170°, $+190^{\circ}$; -185°, $+175^{\circ}$; correspond to identical regions of the astronomical sky. In Table 5-3 we assemble the statistical parameters for the four pairs of observations plus the ensemble of all the data in Table 5-2. We first inspect the correlation coefficients. The writer of this chapter (FER) has been involved in the interpretation of observational data, astronomical and geophysical, for more than forty years and states apodictically that these are the highest correlation coefficients he has ever dealt with. As a matter of fact, the entire case for our judgment that the photometric data of the OSO-6 Rutgers experiment deserve an in-depth study is based on the correlation coefficients of the last column of Table 5-3. The variation in the slopes and intercepts for the four primary cases indicates that some finesse is required in progressive iterations in the interpretation of the observations.

5.4 THE ABSOLUTE CALIBRATION AND ACCURACY OF THE PHOTOMETRIC DATA

The determination of the calibration parameters to convert the linearized readings from OSO-6 into absolute photometric quantities involves all the problems that ground-based observers have had to contend with. The sky provides us with numerous point light sources, the stars, and star crossings constitute a fundamental source of calibration material. We have actually used three different methods in our calibrations: (1) star crossings, (2) comparison of ground-based

Milky Way observations with the satellite observations of the same M. W. regions, (3) comparison of gegenschein photometric gradients, ground-based and space. The three methods all converge to give similar parameters. We shall here give an example of the second method. In Table 5-4 we list the values of the linearized counts from OSO-6 and the ground based measurements of Smith, Roach and Owen (9) for a traverse of the Milky Way which came close to the galactic center direction which we shall later be concerned with in our discussion of colorimetry. Each entry of D530 from OSO-6 is the mean of 30 readings for the six positions of the polarimetric elements (as was also the case in the data of Table 5-2). The data are shown plotted in Figure 5-8. An orthogonal least-squares solution yields the calibration equations:

$$D530 = 87 + 1.657\ S10(vis), \text{ or}$$
$$S10(vis) = -52 + 0.6035\ D530.$$

The correlation coefficient, 0.919, is a measure of the uncertainty in both the ground-based and the satellite observations. It should be noted that in "orthogonal" least-squares solutions neither variable is considered to be "independent" since what is minimized in the solution is the sum of the squares of the residuals measured in a perpendicular direction from the points to the deduced regression line.

The intercept is associated with the fact that the satellite observations include both the Milky Way as the major contributor plus a region about five degrees from the center of the gegenschein whereas the ground data are for integrated starlight only. The intercept could also be involved with uncertainty in making exact allowance for the instrumental "dark current" in the satellite data.

5.5 SOME PUBLISHED PHOTOMETRIC RESULTS.

We shall here summarize some of our published results based on an interpretation of some of the photometric observations of the experiment.

The Gegenschein or Counterglow

In the illustration given under absolute calibrations we used,

as an illustration, a traverse of a bright region of the Milky Way where the integrated starlight is the predominant source of radiation. In order to study the gegenschein we deliberately choose orbital sequences for seasons in which the counter-sun direction is well away from the Milky Way so that the integrated starlight becomes the junior partner and the sunlight scattered by the particles in the counter-sun direction is predominant.

In a paper (reference 7) we have reported on a definitivestudy of the antisun region over a span of 124 orbits, during a period when the observations were oriented toward a part of the sky between the two arms of the Milky Way. The elongations included in the study were -180° (antisun), -170°, -175°, -185°, -190°, and -195°, a total span of 25°, from 10° away from the antisun in one direction to 15° in another. The sequence involved a slice across the gegenschein inclined about 48 with respect to the ecliptic. In Table 5-5 we give a comparison between the mean of the space observations and ground observations, (reference 6). It is seen that the space and ground observations are in substantial agreement.

Reference #8, A Photometric Perturbation of the Gegenschein. This paper reports on a continuation of the methods employed in the previous paper. We found that the gegenschein cannot be assumed to be a constant photometric phenomenon. Over a period of about 60 orbits (orbits 6420 to 6480) there is evidence of a weakening of the brightness in the antisun direction relative to all five of the other elongations. It should be emphaziized that if the effect were the opposite, namely that all the elongations indicated an increase in the -180° brightness, this would be logically interpreted as due to the presence of a bright region in or near -180 such as a star or a group of stars. (we recall that a single star crossing a 2 degree field requires 30 orbits). But a decrease in brightness such as we reported in reference 8 cannot be similarly rationalized and we conclude that the evidence indicated spottiness in the dust cloud contributing to the gegenschein.

REFERENCE #10 COUNTER GLOW FROM THE EARTH-MOON LIBRATION POINTS.

This paper is a logical extension of and continuation of the preceding paper. If, as we have suggested, the dust cloud in the anti-sun direction is not photometrically constant in time, then we should look carefully at a problem that has been actively pursued in the literature over some fifteen years after the Polish astronomer, Kordylewski, raised the question whether there is a slight but measurable enhancement of brightness in the directions of the LaGrangian libration points, L4 and L5, with reference to the Earth-Moon system. According to the analysis by LaGrange, about two centuries ago, there is a special solution of the gravitational three-body problem which results in two quasi-stable regions for small (less massive) bodies which find themselves at the apices of equilateral triangles with respect to two massive bodies and in the orbital plane of same. (actually, LaGrange predicted a total of 5 quasi-stable regions but only the two, L4 and L5, concern us here). These are referred to as quasi-stable regions since small objects are not strictly constrained to the regions but will, in general, perform oscillations around the mathematical points, especially if there are gravitational perturbations from a fourth body (for example from the sun in the case of the Earth-Moon system).

A test of the Kordylewski hypothesis is available to us in the OSO-6 data. During each lunation the observations in the antisun (gegenschein) cap traverse the L4 (preceding) and the L5 (following) regions at lunar elongations of 60 degrees. The tempo of the traverse is that of the moon in its orbit or about 13 degrees per day. From one satellite orbit to the next, the view for a given elongation is 13/15 = 0.9 degree. If a LaGrangian cloud extends over 9 degrees, for example, it would thus be traversed in our experiment in 10 contiguous orbital passages.

The evidence of the paper here being summarized indicates the probable presence of a slight photometric enhancement in the L4 and L5 directions which is about 10% as bright as the gegenschein. Since

the gegenschein is barely visible against the general sky background to an observer under ideal conditions it is to be expected that the visual or even the photographic detection of such a faint perturbation would be extremely difficult. As a matter of fact most attempts to isolate the phenomenon have been unsuccessful and our analysis of the OSO-6 data probably represents a marginally significant result but is included as an honest attempt to measure an elusive phenomenon.

5.6 COLORIMETRY

The basic precision of the photometric data as demonstrated by the correlation coefficients higher than 0.99 (Table 5-3) between observations of the astronomical sky at opposite extremes of a given orbit attests to the internal consistency of the separate sky readings based on a given "reading" as the mean of 30 datum points. The observing procedure was to read said 30 datum points for each of the three color filters. In the sample used to establish the precision the 30 points of one reading corresponded to a mean reading of 1190.8 (5000A) which should result in an inherent precision of about 0.5% (based on the assumption that precision is proportional to the square root of the total reading, in this case 30 x 1190.8 = 35724). For the other two colors the same sample indicated internal precision of 1.1% for wave-length 4000A and 0.8% for 6100A.

With such inherent precision in the three colors we were encouraged to make a systematic colorimetric study of the same reservoir of observations as we used in our photometric studies at a particular color. We shall here report on such a study of the region of the Milky Way surrounding the direction toward the galactic center (to simplify terminology we shall hereafter refer to "the direction toward the galactic center" as simply "the galactic center").

It is convenient to use the conventions which have become universal among astronomers in colorimetric studies, namely the use of "magnitude differences" to indicate colors and color changes. Many "young Turks" over the years have rebelled at the stellar magnitude scale but all rebellions have been abortive and we fall

back on the system. In Table 5-6 we show a comparison of the colors of our equipment which we label b,v,r in comparison with the B,V,R system used by the astronomical fraternity. The standard procedure is to compute the delta magnitudes as follows:

$$B - V = 2.5 \log Rv/Rb + C1$$
$$B - R = 2.5 \log Rr/Rb + C2$$
$$V - R = 2.5 \log Rr/Rv + C3$$

where R is the raw reading for the subscripted color. The C values are empirically determined in the calibration and include differential filter transmissions and photoelectric cathode color sensitivities. The calibration of our filter-photometer combination led to the following equations for our set-up:

$$b - v = 2.5 \log R5000/R4000 - 0.781$$
$$b - r = 2.5 \log R6100/R4000 + 0.894$$
$$v - r = 2.5 \log R6100/R5000 + 1.675$$

The empirical relationship between our colors and the conventional astronomical colors is given by the following equations:

$$b - v = 1.109\ (B-V) + 0.111$$
$$b - r = 1.031\ (B-R) + 0.256$$
$$v - r = 0.937\ (V-R) + 0.122$$

From the effective wave-lengths of our filters we have used the data of Table 5-7 to deduce "color temperatures" from the color indices. We show a series of five plots (Figures 5-9, 5-10, 5-11, 5-12, 5-13) to illustrate the color pattern of the galactic center based on OSO-6 observations. The general photometric maximum in all three colors is away from the galactic center at the following positions:

4000A $\quad b = -6^\circ\ ;\ l = 358^\circ$
5000A $\quad b = -3^\circ\ ;\ l = 3^\circ$
6100A $\quad b = -4^\circ\ ;\ l = 3^\circ$

The color plots portray rather complex patterns. In b-v there

are two red "patches", a large one centered near b = -5 ;l = 2 ; and a small one at b = 2 ; l = 5 . In the v - r plot there is a single red patch at b = 2 , l = 2 .

The significance of these color observations probably lies in the fact that in the three colors we are probing to different distances toward the galactic center in the sense that the longer wave-length probing (6100A) is probably deeper than that for 5000A which in turn probably probes more deeply than 4000A.

5.7 POLARIZATION STUDIES.

The OSO-6 Rutgers experiment was planned with polarization measures of the zodiacal light, both linear and circular, in three colors as a prime objective. Ground-based polarizations measurements had indicated that linear polarizations up to some 20% could be expected at solar elongations of about 60 degrees. But, as we have noted, the hemisphere toward the sun, that is within a solar elongation of 90 degrees, is so affected by scattered sunlight as to contaminate the observations in that domain very seriously. In the gegenschein cap where we have concentrated our analytical attention the linear polarization is presumably very small Let us set a tentative working polarization goal of 1% and examine the possiblity that we can approach this sort of finesse with our data. Using the square root "rule", 1% precision calls for total counts, N, of 10,000 (% = $100\sqrt{N}/N$). In Table 5-8 we show a sample of the 30 individual readings for a typical region well away from the Milky Way. The six columns correspond to the six settings of the polarizing elements in the polarimeter. Before discussing the details of the elements it is instructive to inquire into the potential for significant polarization results from a sample of data such as that of Table 5-8 which is typical of the general situation which we encountered. We note the following:

(1) The total of counts at our disposal was 988

(2) The standard deviation of the means by columns was 7.6 corresponding to 3.9% of the mean (com-

pare this with 100 x $\sqrt{988}/988$ = 3.2%).

(3) Taking the over-all mean of the 30 observations including all six polarization settings we find that the standard deviation of the mean is 1.9% of the mean (compare with 100 x$\sqrt{5329}/5329$ = 1.3%).

In figure 5-14 we show a plot of the means for the six positions with error bars corresponding to the standard deviations together with the over-all mean with its standard deviation indicated by cross hatching.

It is obvious that polarizations based on a sample such as that displayed in Table 5-8 could be considered to be significant if we were dealing with high polarizations in the 20% domain but not useful for polarization studies in the 1% domain. Thus we must abandon any attempt to get significant polarization data from single-orbit observations in the antisun direction for regions well away from the Milky Way such as orbit 6325 of Table 5-3.

In the bright Milky Way the readings are as much as 7 times as large as for orbit 6325 so we can expect to approach columnar precision about the same as we get for the ensemble of 30 observations in orbit 6325 (probably a little better because of possible systematic differences of an instrumental nature between columns to be discussed next). For example if, in the Milky Way, we deal with counts of 1500, then in a column the total of counts is 7500 and the expected precision is approximately 100 x $\sqrt{7500}/7500$ = 1.2%. This could yield a meaningful analysis of the data if the natural polarizations were several percent but marginal for even the Milky Way where again we anticipate that our search will be in the vicinity of 1% polarization.

Before continuing with a discussion of the inherent precision of our data we should go into the matter of the details of linear polarization calculations based on the relationships among the six columnar entries. In Table 5-9 we show the nature of the polarizing elements introduced into the optical path corresponding to the six

columns.

All four Stokes parameters can be determined from the six settings but we have concentrated largely on the problem of the linear polarization which involves the first four positions (columns). (A small amount of effort has been expended on the problem of circular polarization involving the 5th and 6th positions). Any systematic difference in the readings for positions 3 and 4 relative to 1 and 2 will introduce an instrumental spurious polarization. Thus we are concerned that figure 5-14 suggests that positions (columns) 3 and 4 give systematically lower readings than 1 and 2. The physical explanation may lie in the fact that there are two rotators in the optical path for positions 3 and 4 and only one in positions 1 and 2 (Table 5-9).

Our analysis of the basic data on inherent precision and on the systematic effects mentioned in the previous paragraph is the rationale for our procedure in attempting to glean significant linear polarization data from the OSO-6 observations.

(1) We have concentrated on changes in polarization patterns on the assumption that any constant polarization could be instrumental,

(2) We have adopted severe smoothing techniques over many orbits in order to increase the effective counts but in so doing have had to sacrifice resolution.

The Smoothing Technique

Our procedure is to do a double smoothing:

(1) We took running means of the readings in a given column over 7 contiguous orbits.

(2) We took running means of the deduced polarization elements by 5's.

The net result was to increase the effective counts entering, into a final value of

$$7 \times 5 \times 1000 = 35000 \text{ counts.}$$

Thus each columnar value had an effective precision of

$$100 \times \sqrt{35000}/35000 = 0.5\%$$

This procedure limited the resolution of the final results effectively to seven orbits at best, but since the sidereal sky requires about 30 orbits to traverse the photometer's field of two degrees we have accepted the restriction on the resolution.

In Figures 5-15 and 5-16 we show two results for wave-length 5000A based on the above smoothing procedure. Figure 5-15 shows graphically the E-vector for a sample of 60 orbits at a solar elongation of 185 degrees. Figure 5-16 illustrates the E-vector polarization for 200 contiguous orbits and 6 solar elongations. The samples are taken for a time when the antisolar cap was far from the Milky Way so the results refer predominantly to the back-scattered sunlight from interplanetary particles.

The empirical features brought out by the figures are (1) linear polarizations above the instrumental level of 0.5% are indicated and (2) the time and / or space variations in the length and orientation of the E-vectors display complex patterns. The patterns for elongations separated by 5 degrees do not in general correlate. If the effective distance of the material responsible for the patterns is that of the moon then the spatial perturbations must be smaller than about 35,000 kilometers. Treating the patterns as a time phenomenon, for example as due to clumps of polarizing material sweeping radially outward through the solar system, we arrive at an extent corresponding typically to, say, 20 orbits or 30 hours of time. The linear extent implied depends on the assumed speed of radial movement of the speculative cloud. For example, a speed of 100 km/sec corresponds to an extent of 30 x 3600 x 100 = 11 million kilometers or about 0.11 astronomical unit.

SUMMARY

We have outlined the three types of analysis to which we have subjected the data from the Rutgers experiment on OSO-6: (1) photometry (2) colorimetry and (3) polarimetry. We have indicated the restrictions placed on the analysis due to the interdiction of much of

the data (1) from scattered light originating in light sources within 90 degrees of the line of sight and (2) from the numerical level of the counts available to us in the observable reservoir of data.

A further restriction was imposed by the fact that we gave full diagnostic treatment to about 8,000 of the 14,000 orbits of data, about 57% of the total. Future investigations should concentrate on the balance of the data particularly since a second crossing of the galactic center would then be at our disposal. The colorimetry of this important part of the Milky Way should be repeated by a study of the traverse in the undigested orbits. Extended study of the elusive libration clouds would also be possible by such a continued effort.

REFERENCES

1. A. L. Rouy and L. H. Aller, A Feasibility Study Of A Radiation Analyzer For The Zodiacal Light, NsG 550, Rutgers, the State University,Newark, New Jersey, March, 1964.

2. A. L. Rouy, B. Carroll and L. H. Aller, Experiment For The Determination Of The Brightness, Polarization and Ellipticity Of The Zodiacal Light From The OSO-F, NsG 550, Rutgers, the State University, Newark, New Jersey, October, 1965.

3. B. Carroll and F. E. Roach, Preliminary Report On The OSO-G Rutgers Zodiacal Light Experiment, Rutgers, the State Universiyy, July 10, 1970.

4. Ball Brothers Research Corporation, Final Report, # 70-11, Rutgers Zodiacal Light Analyzer For OSO-G.

5. A. Rouy, B. Carroll, L. H. Aller, F. E. Roach and L. L. Smith, Measurements Of The Gegenschein From Space, Nature, 232, 323, 1971.

6. F. E. Roach, A Photometric Model Of The Zodiacal Light, Astr. Jnl., 77, 837, 1972.

7. F. E. Roach, B. Carroll, L. H. Aller and J. R. Roach, A Photometric Study Of The Counterglow From Space, Planet. Space Sci., 21, 1179, 1973.

8. F. E. Roach, B. Carroll, J. R. Roach and L.H. Aller, A Photometric Perturbation Of The Counterglow, Planet. Space Sci., 21, 1185, 1973.

9. L. L. Smith, F. E. Roach and R. W. Owen, A Photometric Map Of The Milky Way, Battelle Northwest Report, BNWL-1419, UC-2, 1970.

10. J. R. Roach, Counterglow From The Earth-Moon Libration Points, Planet. Space Sci., 23, 173, 1975.

11. F. E. Roach, B. Carroll, L. H. Aller and J. R. Roach, The Linear Polarization Of The Counterglow Region; in the book: Planets, Stars and Nebulae Studied with Photopolarimetry, pages 794-803, the University of Arizona Press, 1974.

12. J. R. Roach, The Color Of The Libration Point Countergow, paper presented at the I.A.U. colloquium in Heidelberg, 1975.

13. F. E. Roach and Janet L. Gordon, The Light Of The Night Sky; book published by Reidel (Holland), 1973..

14. F. E. Roach, The Light Of The Night Sky; paper presented at International Astrophysical Conference at Liege, Belgium, 1975, to be published in the Conference Proceedings.

15. F. E. Roach and C. F. Lillie, Comparison Of Surface Brightness Measurements From OAO-2 And OSO-6; NASA Report SP-310, pages 71-79, 1972.

16. F. E. Roach, B. Carroll, L. H. Aller aqn L. L. Smith, Surface Photometry Of Celestial Objects From A Space Vehicle; Proc. National Academy of Sciences, 69, 694, 1972.

TABLE 5-1

SCATTERED LIGHT BASED ON LUNAR OBSERVATIONS

ANGLE FROM AXIS	RELATIVE RESPONSE	LOG RELATIVE RESPONSE
0.0	1.0	0.00
0.5	0.89	- 0.051
1.0	0.805	- 0.094
1.5	0.46	- 0.319
2	0.252	- 0.599
3	0.151	- 0.821
4	0.091	- 1.042
5	0.055	- 1.262
6	0.033	- 1.49
7	0.019	- 1.71
8	0.012	- 1.90
9	0.0076	- 2.12
10	0.0053	- 2.27
11	0.0029	- 2.54
12	0.0021	- 2.68
13	0.0015	- 2.84
60-90	10 (-10)*	-10

* Estimated from solar observations

TABLE 5-2

LINEAR COUNTS OF PAIRED OBSERVATIONS

5000A

ORBIT NUMBER	ELONGATION ANGLE							
	-180°	+180°	-175°	+185°	-170°	+190°	-185°	+175°
4780	630	679	736	645	717	612	535	597
4781	628	650	752	643	715	606	570	578
4782	623	668	743	630	706	588	550	561
4783	630	673	745	650	694	602	506	564
4784	644	692	760	690	709	625	506	547
4786	695	737	826	709	777	666	530	591
4787	717	770	855	741	789	680	542	606
4788	754	787	872	763	806	713	551	622
4789	782	803	889	781	827	726	558	627
4790	776	826	911	804	850	754	556	656
4791	812	821	957	834	886	780	582	643
4792	829	856	972	852	903	797	592	659
4794	882	940	1011	900	950	835	616	692
4795	923	953	1017	890	949	826	627	673
4796	945	1007	1032	931	957	850	636	673
4797	990	1052	1074	987	960	872	615	682
4798	1005	1019	1106	1028	986	900	640	699
4800	1004	1056	1174	1071	1038	943	655	732
4802	1039	1045	1307	1098	1137	978	709	758
4803	1020	1056	1288	1135	1150	1007	736	788
4804	1020	1067	1334	1158	1224	1054	737	795
4805	1024	1046	1380	1239	1254	1146	773	845
4806	1007	1041	1441	1278	1346	1194	792	870
4807	994	1056	1472	1327	1368	1241	806	897
4808	1026	1054	1545	1348	1449	1241	828	925
4809	978	1012	1557	1366	1465	1268	839	932
4810	949	992	1575	1383	1462	1283	861	924
4811	941	972	1585	1394	1442	1255	880	924
4812	914	937	1585	1454	1382	1235	843	901
4814	902	927	1624	1417	1399	1221	860	927
4815	916	926	1646	1450	1415	1206	886	961
4817	896	925	1688	1474	1408	1241	905	957
4818	923	936	1723	1491	1442	1217	914	985
MEAN	873	908	1187	1047	1078	944	689	751
r	.993		.996		.996		.991	
a	44.7		-5.0		-3.1		26.7	
b	.989		.886		.879		1.052	

TABLE 5-3

ORTHOGONAL LEAST SQUARES SOLUTIONS

ELONGATIONS (deg)

x	y	a	b	r
-180	+180	44.7	0.989	0.993
-175	+135	- 5.0	0.886	0.996
-170	+190	- 3.1	0.879	0.996
-185	+175	26.7	1.052	0.991
All data		167	0.780	0.961

$y = a + bx$

r = correlation coefficient

TABLE 5-4
LINEAR COUNTS (OSO-6) AND GROUND OBSERVATIONS , S10(vis)
ELONGATION = -175 DEGREES

5000A

ORBIT NUMBER	D530	S10(vis)	ORBIT NUMBER	D530	S10(vis)	ORBIT NUMBER	D530	S10(vis)
4489	199	103	4717	634	271	4929	895	587
4500	170	105	4719	606	262	4930	890	539
4490	201	103	4732	618	284	4944	805	546
4515	200	116	4748	621	289	4945	769	545
4531	282	125	4750	635	284	4959	785	543
4535	287	133	4751	661	289	4960	772	541
4546	336	135	4756	607	289	4975	897	537
4550	342	150	4757	637	284	4976	877	537
4562	526	155	4780	736	404	4990	699	521
4565	544	194	4792	972	598	4991	697	521
4577	603	197	4746	619	289	5005	964	464
4580	604	205	4805	1380	519	5006	959	467
4593	575	204	4806	1441	525	5020	800	425
4595	579	214	4807	1472	804	5021	813	378
4599	734	214	4832	1575	962	5022	741	375
4610	599	261	4836	1650	953	5035	546	388
4626	614	242	4838	1693	911	5039	516	385
4641	631	217	4851	1562	882	5051	619	367
4642	623	222	4853	1633	842	5055	557	362
4650	655	222	4866	1485	959	5066	497	316
4656	679	249	4867	1491	891	5067	497	317
4657	678	227	4868	1476	892	5070	482	308
4671	695	311	4882	1324	924	5077	452	306
4672	693	260	4883	1337	832	5081	458	315
4673	697	302	4898	1337	628	5082	443	315
4682	667	343	4913	1098	590	5093	463	312
4686	670	351	4914	1080	607	5094	484	319
4688	677	357	4975	897	537	5096	465	303
4701	662	312	4923	907	625	5111	460	270
4703	663	308	4924	918	606			

TABLE 5-5

GEGENSCHEIN OBSERVATIONS

ANTISOLAR ANGLE	GROUND	SPACE
0	1.000	1.000
5	0.900	0.880
10	0.828	0.791
15	0.778	0.761

TABLE 5-6

COMPARISON OF THE OSO-6 COLOR FILTERS AND THE STANDARD ASTRONOMICAL FILTERS

ASTRONOMICAL STANDARD	OSO -6	PEAK WAVELENGTH (ANGSTROMS)
	b	4000
B		4400
	v	5000
V		5500
	r	6100
R		7000

TABLE 5-7

COLOR TEMPERATURE AND OSO-6 COLOR INDICES

COLOR TEMPERATURE	b - v	b - r	v - r
2000	3.141	5.382	2.241
3000	1.841	3.147	1.306
3500	1.471	2.507	1.031
4000	1.194	2.032	0.838
5000	0.806	1.368	0.562
6000	0.549	0.930	0.381
7000	0.371	0.625	0.254
8000	0.236	0.399	0.163
9000	0.136	0.229	0.093
10000	0.058	0.097	0.039
11000	0.000	0.000	0.000
12000	-0.057	-0.096	-0.039
14000	-0.135	-0.228	-0.093
16000	-0.193	-0.323	-0.130

TABLE 5-8

A TABULATION OF LINEAR DATA COUNTS

ORBIT NUMBER 6325; ELONGATION -180 DEGREES; COLOR : 5000A

	1	2	3	4	5	6
	194	215	199	179	235	202
	226	189	162	169	196	162
	212	194	207	207	189	212
	218	218	184	181	189	238
	210	194	215	153	194	186
Total	1060	1010	967	889	1003	1000
Mean	212.0	202.0	193.4	177.8	200.6	200.0
Sigma (x)	10.9	12.0	18.6	17.6	17.4	25.4
Sigma(x,mean)	4.9	5.4	8.3	7.9	7.8	11.4
Sigma(x,mean,%)	2.3	2.7	4.3	4.4	3.9	5.7

Over all mean 197.6

Sigma of single reading 20.8

Sigma of mean = 3.8 = 1.9%

TABLE 5-9

OSO-6 POLARIZING ELEMENTS

POSITION	WHEEL 1	WHEEL 2	EFFECTIVE ANALYZER PASS AXIS*
1	-45° rotator	clear	0°
2	+45° rotator	clear	+90°
3	+45° rotator	+45° rotator	+45°
4	-45° rotator	+45° rotator	-45°
5	-45° rotator	1/4 wave plate	
6	+45° rotator	1/4 wave plate	

* With respect to spin axis.

Scattered light in the OSO-6 system based on lunar observations

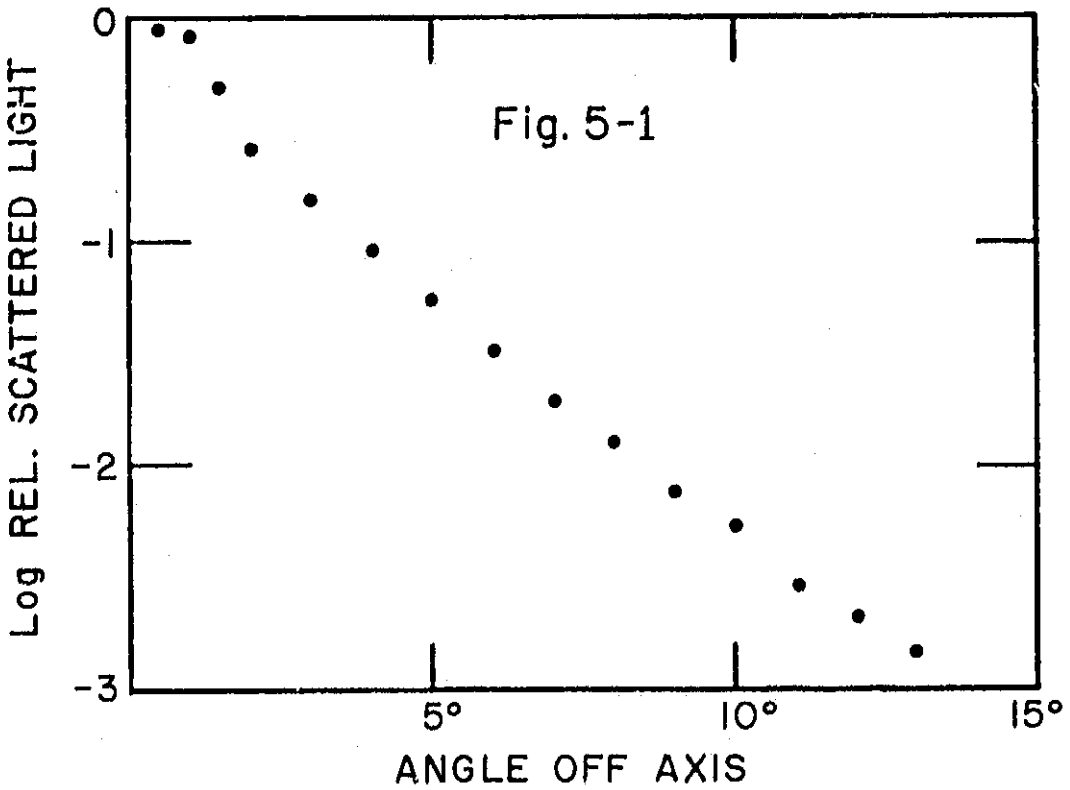

Fig. 5-1

Scattered light in the OSO-6 system based on lunar and solar observations

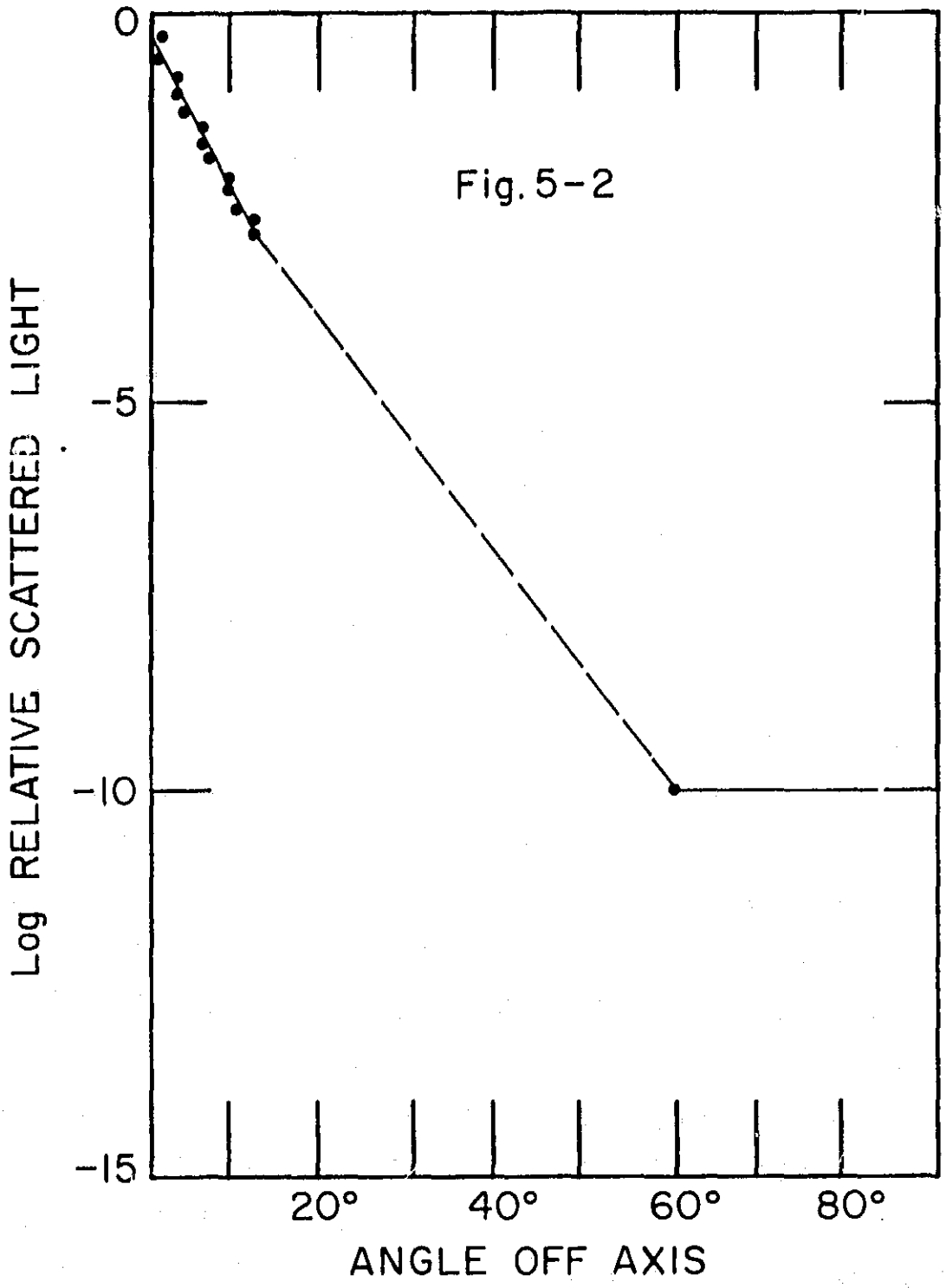

Fig. 5-2

Illustration of paired "morning" and "evening" orientations which observe the same astronomical sky.

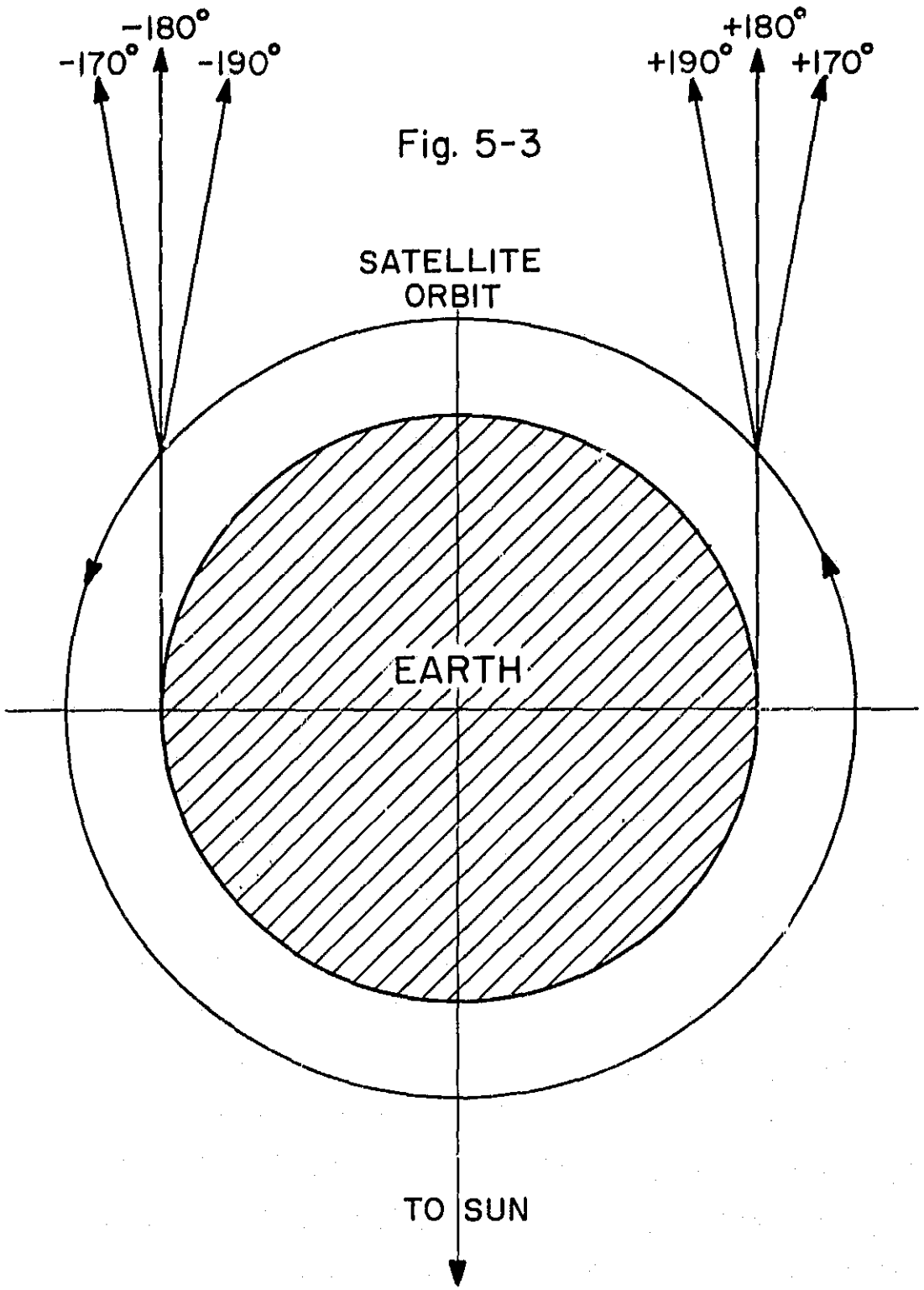

Fig. 5-3

Correlation plot of paired observations:
Elongations -180° and +180°

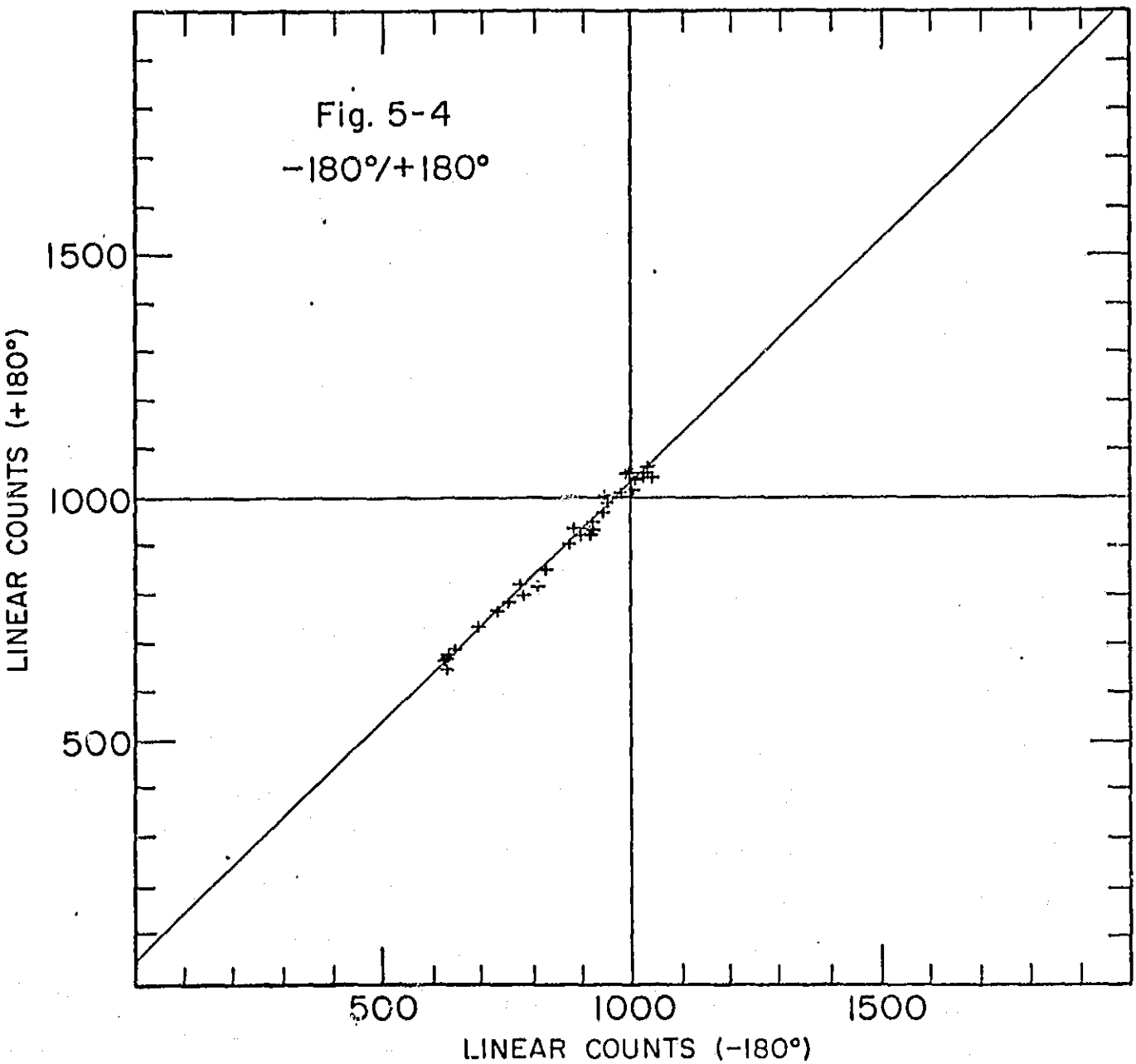

Correlation plot of paired observations: Elongations -175° and +185°

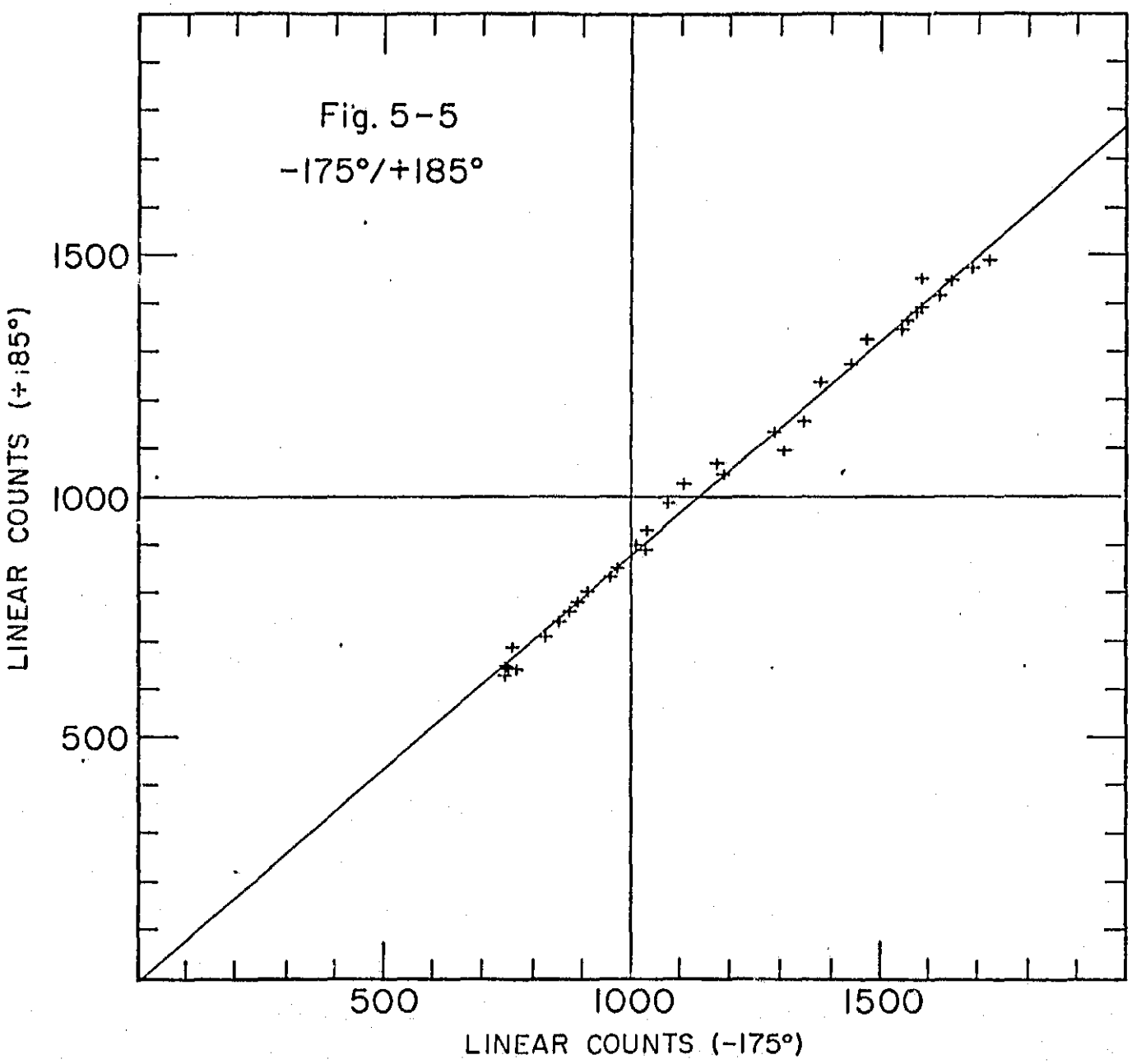

Correlation plot of paired observations: Elongations -170° and +190°

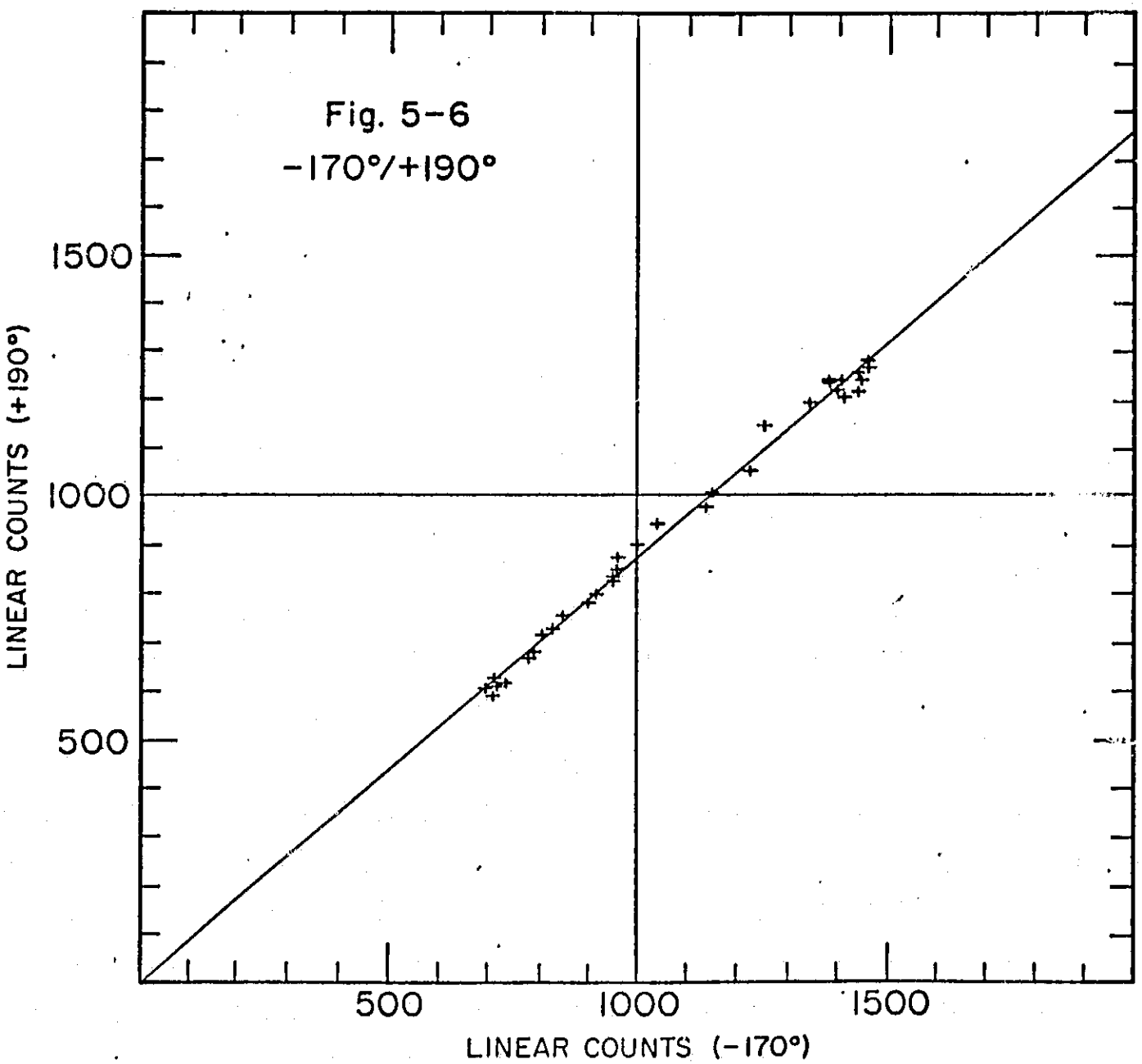

Correlation plot of paired observations: Elongations -185° and +175°

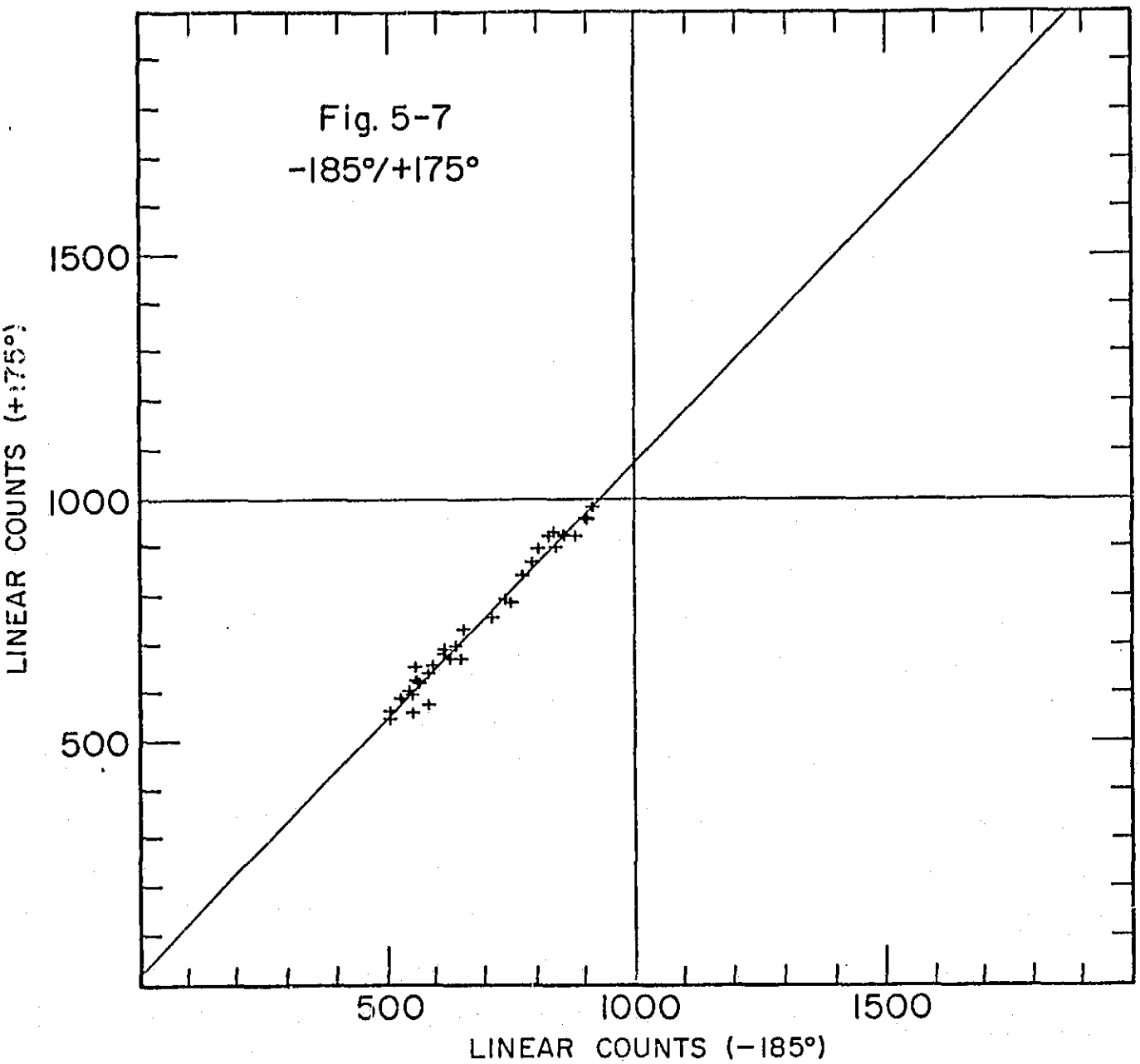

Correlation plot of paired observations: Elongations -185° and +175°

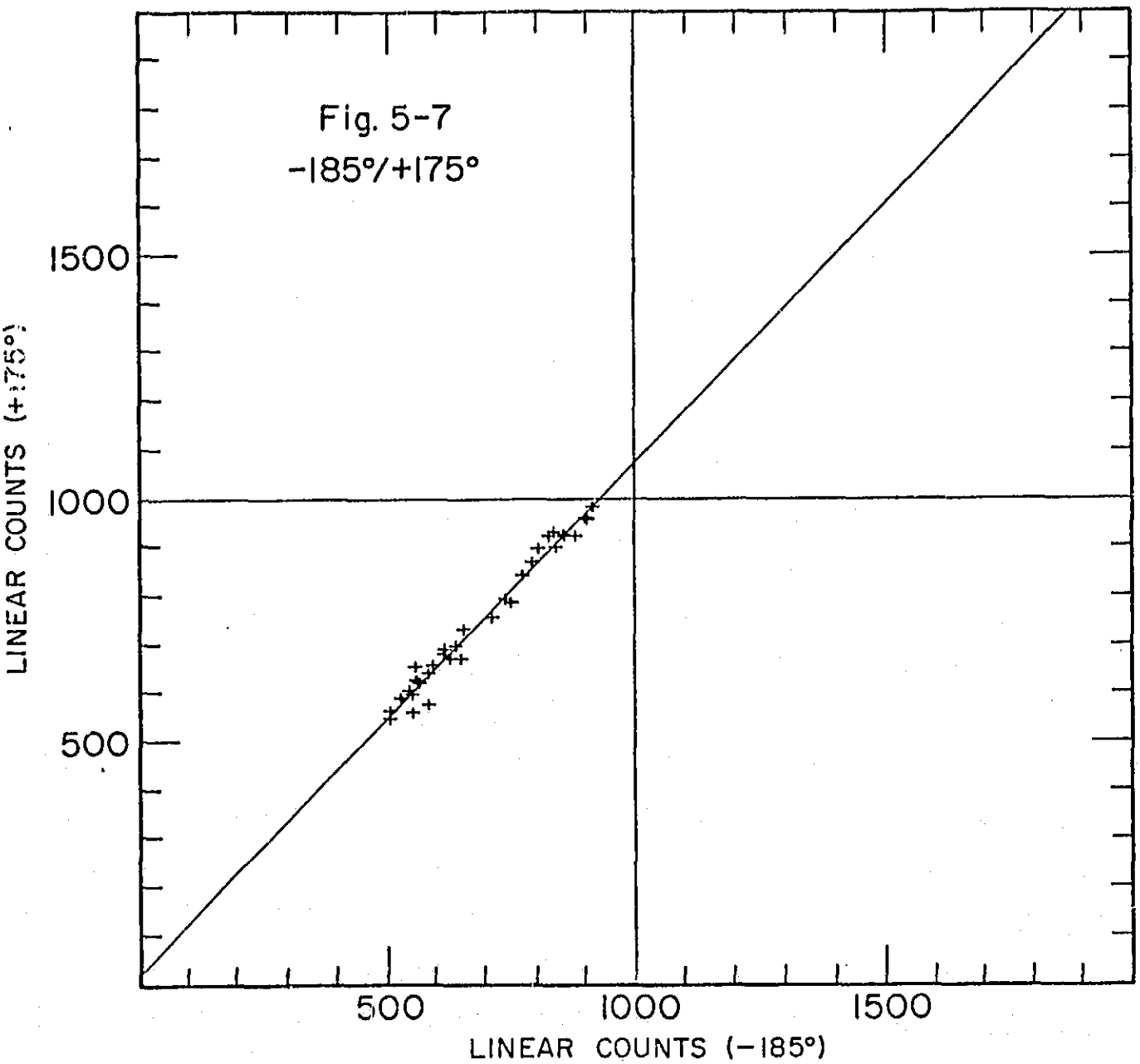

Calibration plot: D530 (OSO-6) versus S10 (vis) from ground observations

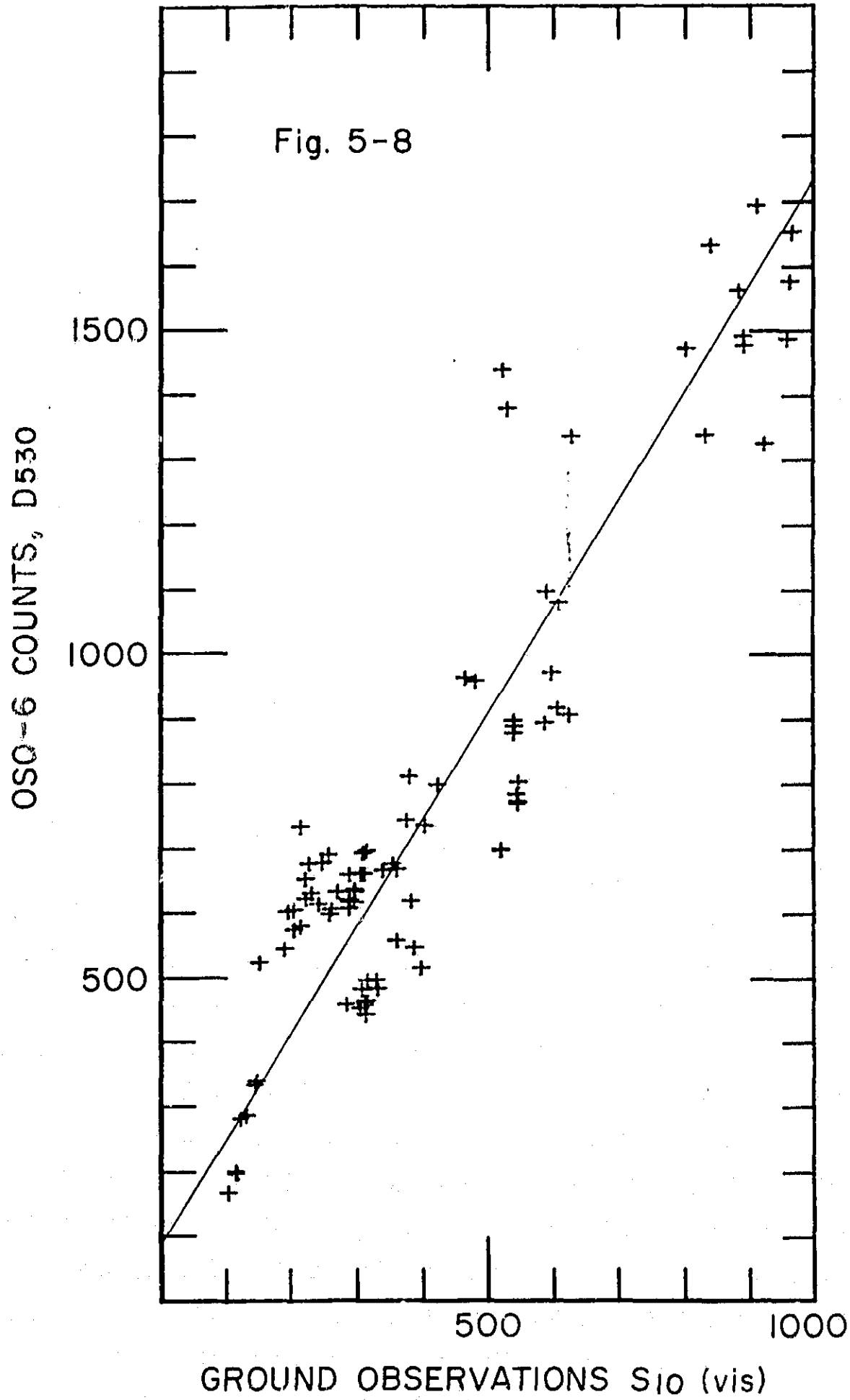

Figure 5-9. Isophotal plot of galactic center region (4000A)

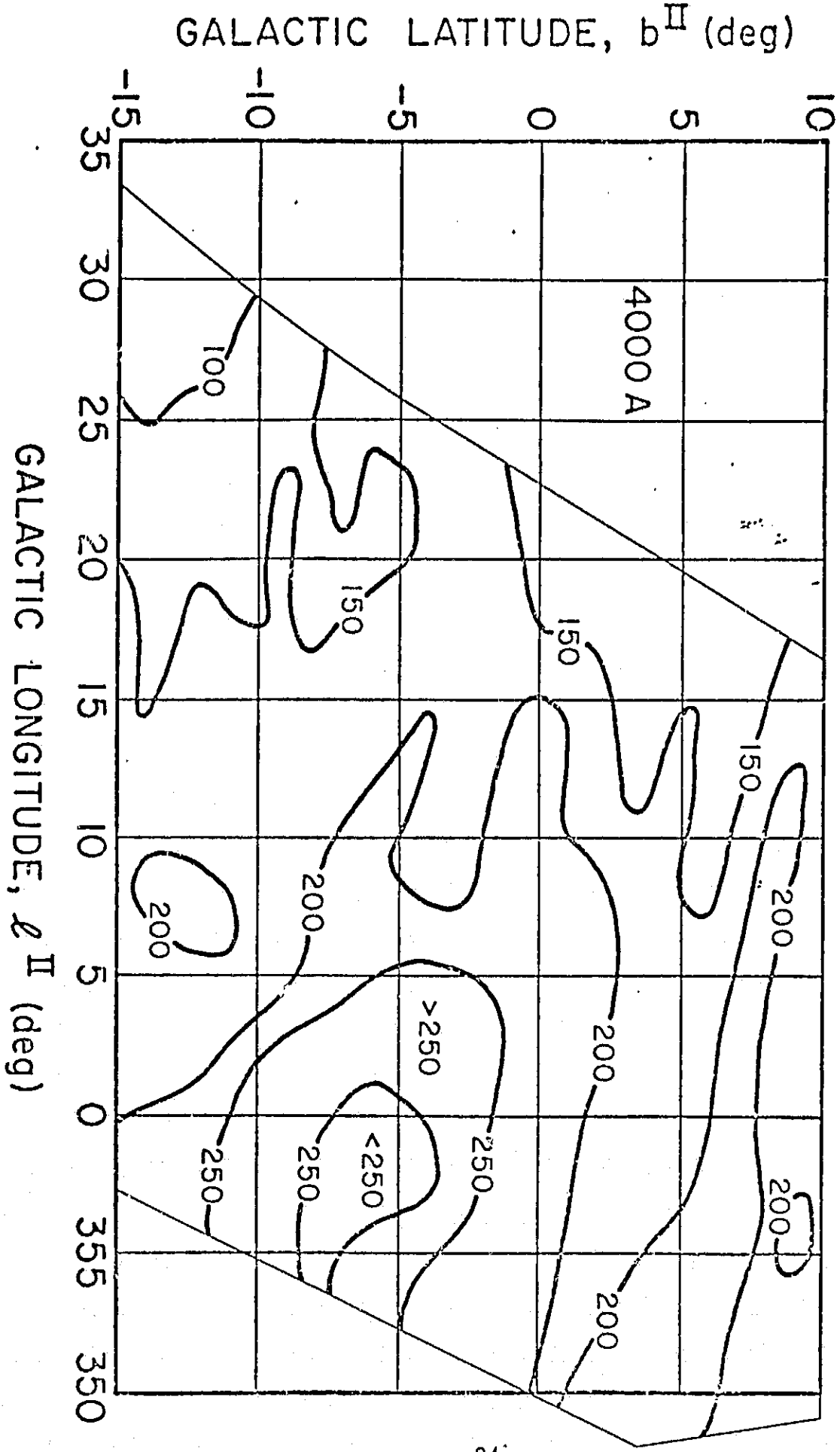

Figure 5-10. Isophotal plot of galactic center region (5000A)

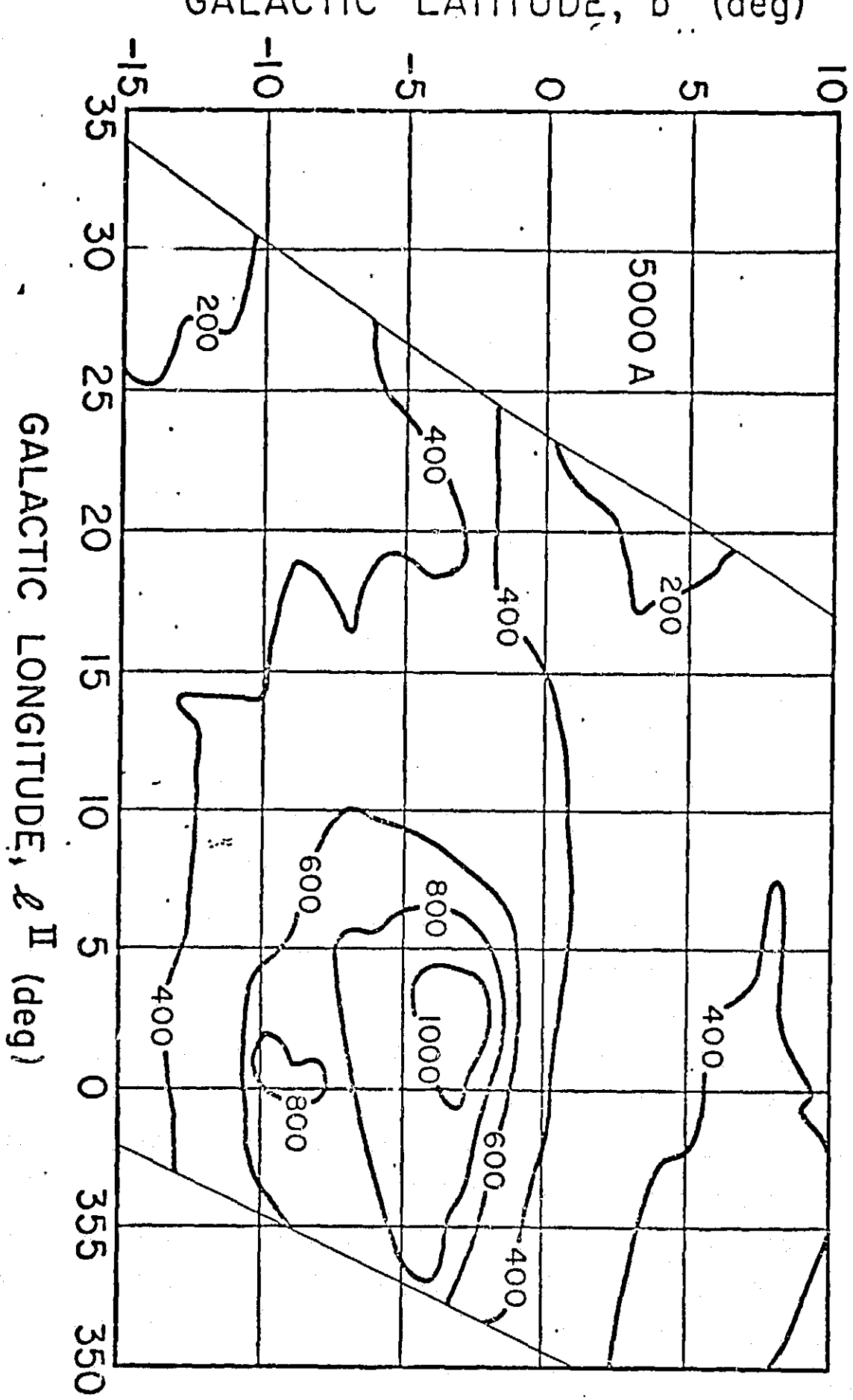

Figure 5-11. Isophotal plot of galactic center region (6100A)

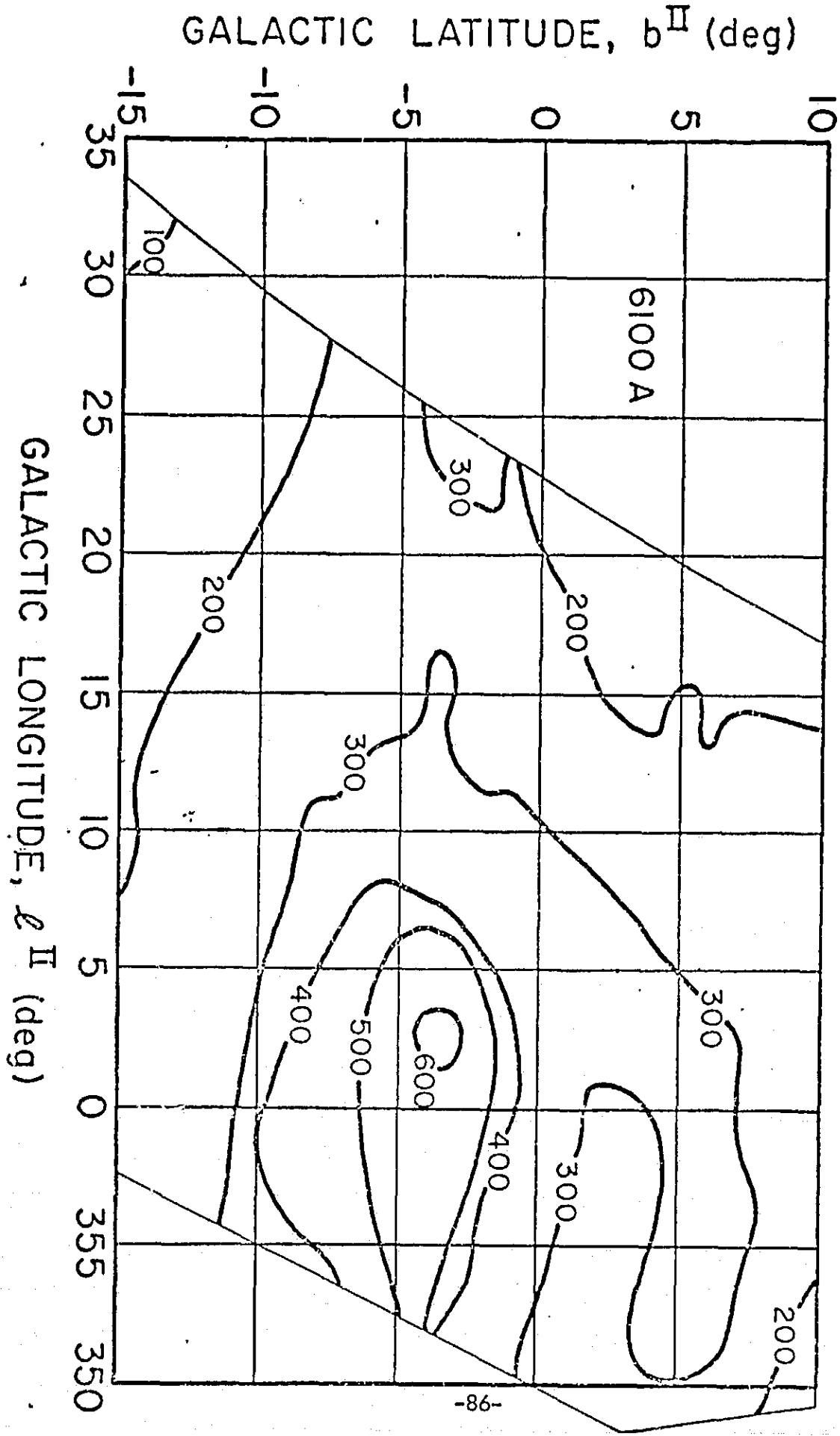

Figure 5-12. Color plot, b-v, for the galactic center region

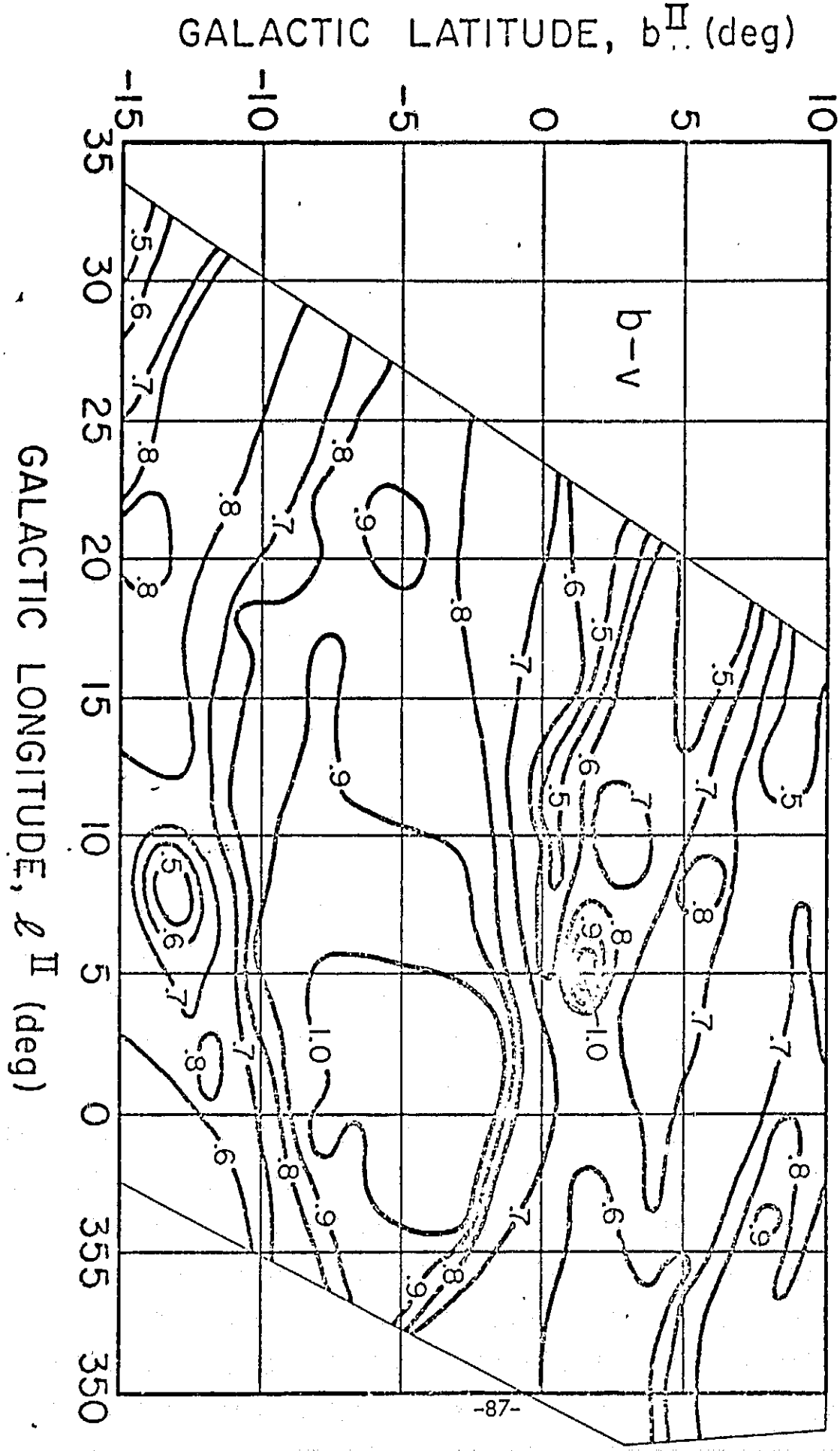

Figure 5-13. Color plot, v-r, for the galactic center region.

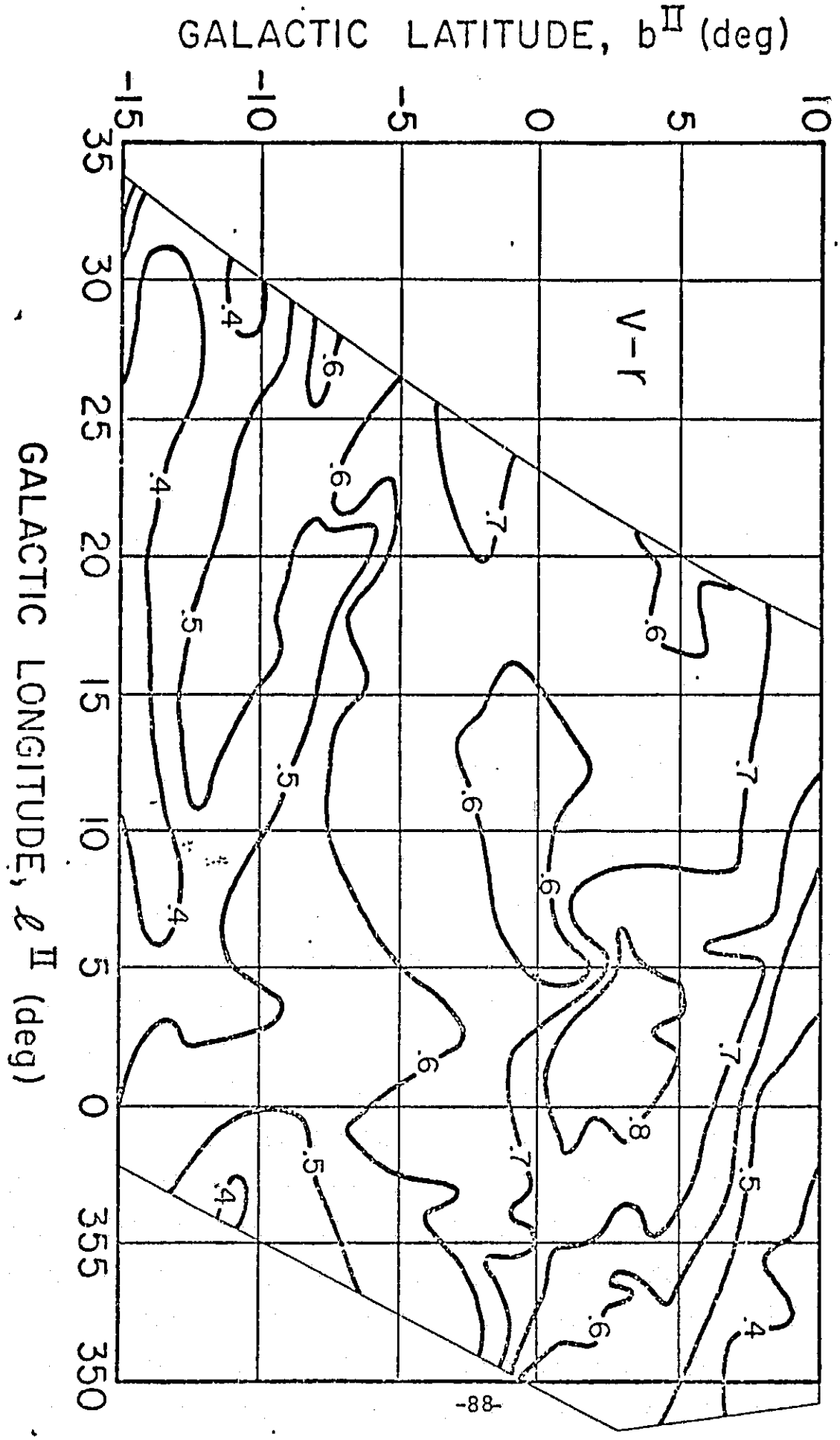

Figure 5-14. Linear counts for the six positions of the polarizing elements, based on data in Table 5-8

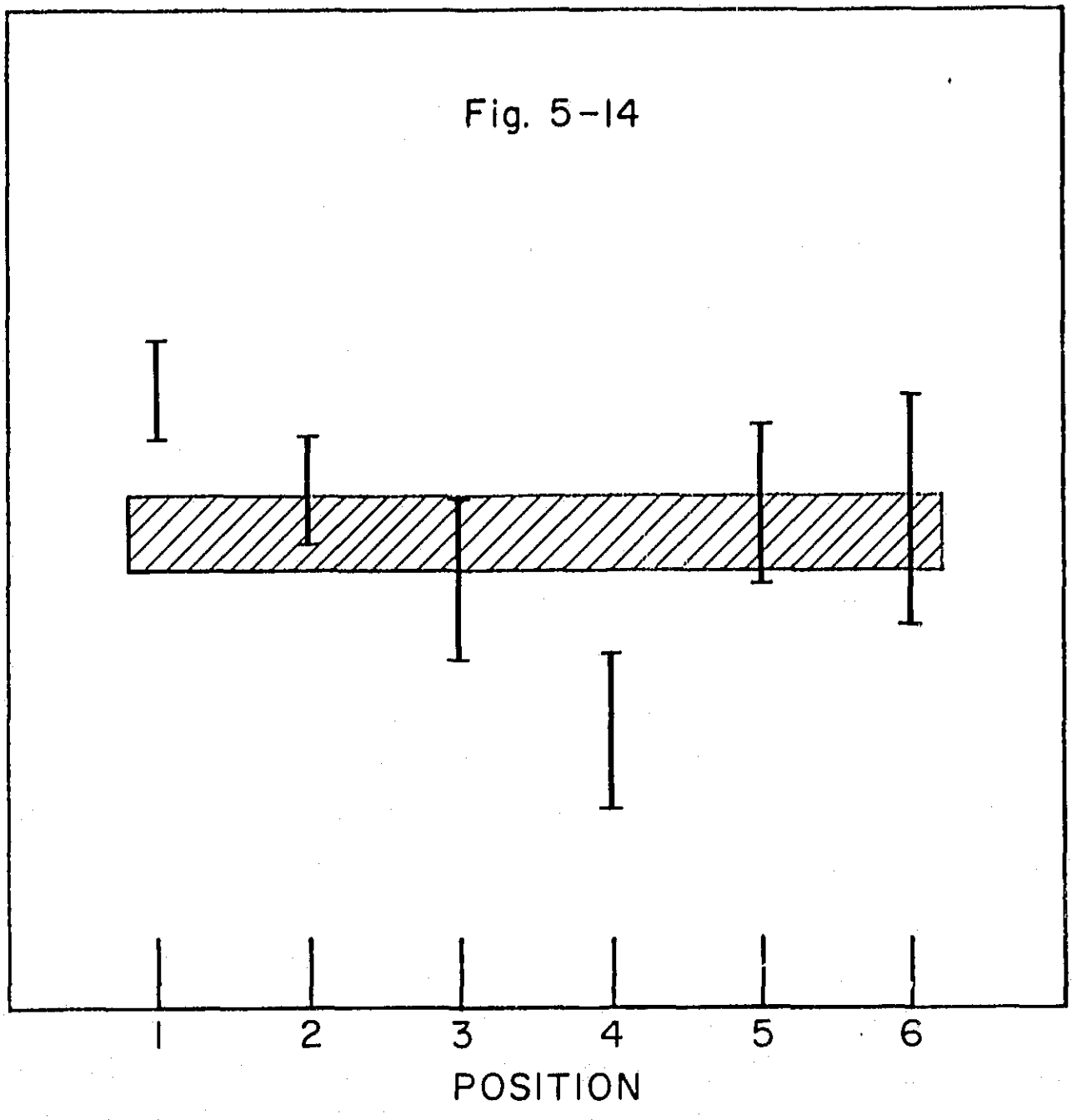

Figure 5-15. Plot of the polarization E-vector in the gegenschein region showing changes over a span of 60 orbits

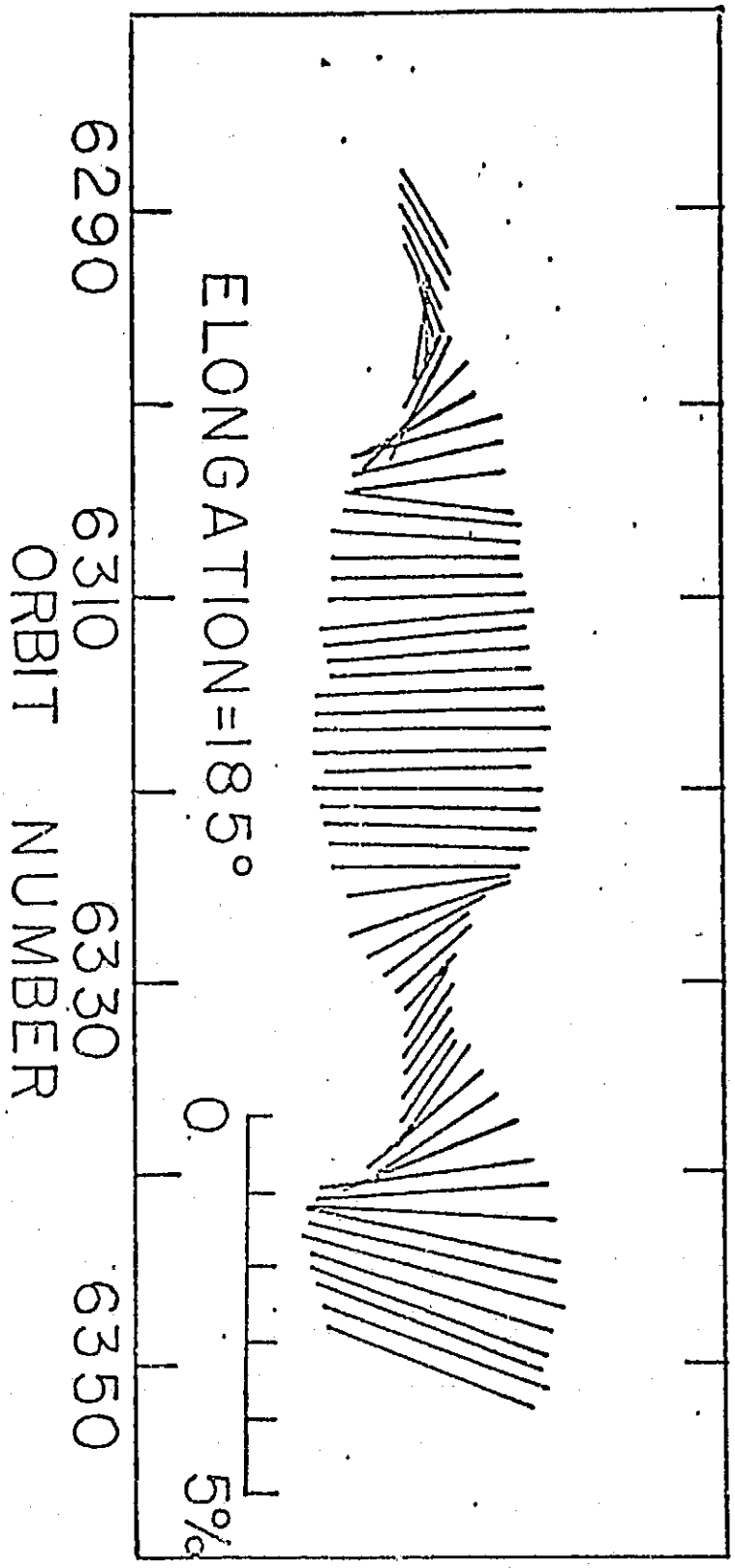

Figure 5-16. Plot of the polarization E-vector for six elongations in the gegenschein cap over a span of 195 orbits